ÇUKUROVA UNIVERSITY
INSTITUTE OF NATURAL AND APPLIED SCIENCES

MSc THESIS

Fatih YILMAZ

THE EVALUATION OF MECHANICAL PROPERTIES OF CYLINDRICAL TEMPERED BARS UNDER QUENCHING CONDITIONS

DEPARTMENT OF MECHANICAL ENGINEERING

ADANA, 2015

ÇUKUROVA UNIVERSITY
INSTITUTE OF NATURAL AND APPLIED SCIENCES

THE EVALUATION OF MECHANICAL PROPERTIES OF CYLINDRICAL TEMPERED BARS UNDER QUENCHING CONDITIONS

Fatih YILMAZ

MSc THESIS

DEPARTMENT OF MECHANICAL ENGINEERING

We certify that the thesis titled above was reviewed and approved for the award of degree of the Master of Science by the board of jury on 06/07/2015.

…….....	…….	…...……...
Assoc. Prof. Dr. Hasan SERİN	Asst. Prof. Dr. Durmuş Ali BİRCAN	Asst. Prof. Dr. Ertaç HÜRDOĞAN
SUPERVISOR	MEMBER	MEMBER

This MSc Thesis is written at the Department of Institute of Natural And Applied Sciences of Çukurova University.
Registration Number:

Prof. Dr. Mustafa GÖK
Director
Institute of Natural and Applied Sciences

Not: The usage of the presented specific declerations, tables, figures, and photographs either in this thesis or in any other reference without citiation is subject to "The law of Arts and Intellectual Products" number of 5846 of Turkish Republic

ABSTRACT

MSc THESIS

THE EVALUATION OF MECHANICAL PROPERTIES OF CYLINDRICAL TEMPERED BARS UNDER QUENCHING CONDITIONS

Fatih YILMAZ

ÇUKUROVA UNIVERSITY
INSTITUTE OF NATURAL AND APPLIED SCIENCES
DEPARTMENT OF MECHANICAL ENGINEERING

Supervisor : Assoc. Prof. Dr. Hasan SERİN
Year : 2015, Pages: 65
Jury : Assoc. Prof. Dr. Hasan SERİN
: Assoc. Prof. Dr. Ertaç HÜRDOĞAN
: Asst. Prof. Dr. Durmuş Ali BİRCAN

The overall objective of this study was to investigate the effects of relative water velocity and water temperature on yield strength and tensile strength applied on continuous quenching process during production of ribbed rebar steel. The first study same quality and size ribbed rebar steel was quenched on different season to provide different water temperatures. The second study quenching was performed in different relative water velocity by changing water volume flow rate. In both studies, the results yield and tensile strength was measured according to ASTM A370 standard. Difference in cooling rate was changed the amount of martensitic structure in the steel and this was affected on the yield and tensile strength of steel.

Key Words: Continuous quenching, Tempering, Rebar, Yield strength, Tensile strength

ÖZ

YÜKSEK LİSANS TEZİ

TEMPERLENMİŞ SİLİNDİRİK ÇELİK ÇUBUKLARIN FARKLI SU VERME DURUMLARI ALTINDA MEKANİK ÖZELLİKLERİNİN DEĞERLENDİRİLMESİ

Fatih YILMAZ

ÇUKUROVA ÜNİVERSİTESİ
FEN BİLİMLERİ ENSTİTÜSÜ
MAKİNA MÜHENDİSLİĞİ ANABİLİMDALI

Danışman : Doç. Dr. Hasan SERİN
Yıl : 2015, Sayfa: 65
Jüri : Doç. Dr. Hasan SERİN
: Yrd. Doç. Dr. Ertaç HÜRDOĞAN
: Yrd. Doç. Dr. Durmuş Ali BİRCAN

Bu çalışmanın genel amacı nervürlü inşaat demiri üretimi sırasında uygulanan sürekli su verme işleminde bağıl su hızı ve su sıcaklığının malzeme akma ve çekme mukavemeti üzerindeki etkisini araştırmaktır. Birinci çalışmada farklı su sıcaklıkları sağlamak için farklı mevsimlerde aynı kalite ve ebatta çeliğe su verme işlemi uygulanmıştır. İkinci çalışmada ise su debileri değiştirilerek farklı bağıl su hızlarında su verme işlemi yapılmıştır. Her iki çalışmada da Sonuçlar ASTM A370 standardına göre akma ve çekme mukavemetleri ölçülmüştür. Soğuma hızındaki fark çelik içerisindeki martenzitik yapı miktarını değiştirmiş ve çeliğin akma ve çekme mukavemetini etkilemiştir.

Anahtar Kelimeler: Sürekli su verme, Temperleme, İnşaat çeliği, Akma mukavemeti, Çekme mukavemeti

ACKNOWLEDGEMENTS

I gratefully thank to my supervisor Assistant. Prof. Dr. Hasan SERİN, for his supervision guidance, encouragements, patience, motivation, useful suggestions and his valuable time spared for the development of this work.

I would like to thank my manager Kadir KARA and my deputy manager İhsan TAŞTEKİN for their continuous support.

Last, special thanks to my family for their absolute support.

CONTENTS **PAGE**

ABSTRACT.....I
ÖZ..... II
ACKNOWLEDGEMENTS III
CONTENTS IV
LIST OF TABLES VI
LIST OF FIGURES VIII
LIST OF ABBREVIATIONS AND NOMENCULATURE X
1. INTRODUCTION.....1
2. LITERATURE REVIEW….....3
3. MATERIAL AND METHOD……...13
3.1. QUENCHING PROCESS……..13
3.1.1. CONTINUOUS QUENCHING…….....…….....26
3.1.2. CONTINUOUS QUENCHING PIPES……...38
3.2. HOT ROLLED REBAR AND STANDARDS……..…38
3.2.1. OVERVIEW OF REBAR STANDARTS……...38
3.2.2. USED REBAR STANDART……..…….39
3.3. MEASURING DEVİCES ……..……..….42
3.3.1. VELOCITY MEASUREMENT OF LIQUID……..…42
3.3.2. TEMPERATURE MEASUREMENT OF STEEL BAR…….....44
3.3.3. TEMPERATURE MEASUREMENT OF LIQUID……....45
3.4. MECHANICAL TESTING…….……...47
4. RESULTS AND DISCUSSION.....49
4.1. DIFFERENT INITIAL LIQUID TEMPERATURE RESULTS……....49
4.2. DIFFERENT RELATIVE LIQUID VELOCITY RESULTS……53
5. CONCLUSION…….……59
5.1. CONCLUSIONS……..……..59
5.2. RECOMMENDATIONS FOR FUTURE WORKS……...60
6. REFFERENCES..... 61

LIST OF TABLES **PAGE**

Table 3.1. Comporation of Typical Properties: QBT vs. Fully Alloyed A615, Grade 60 Rebar……...36
Table 3.2. Chemical Requirements of World Rebar Standards…….....39
Table 3.3. ASTM A 615 USA rebar steel standards ……...….....41
Table 3.4. Specification of the pyrometer …….…….....44
Table 4.1 Constant values for GR60 rebar steel ……..….. 50
Table 4.2 Experiment results for different initial liquid temperature……...…….. 51
Table 4.3 Constant values for GR60 rebar steel ……...…….. 54
Table 4.4 Experiment results for different relative liquid velocities……..……. 56

LIST OF FIGURES **PAGE**

Figure 3.1. Micro Structure Transformations 15
Figure 3.2. Schematic diagram showing a possible sequence of step during the development of cellular precipitation..... 16
Figure 3.3. Pearlite colony advancing into an austenite grain.....16
Figure 3.4. Schematic representation of the microstructures for an iron-carbon alloy of eutectoid composition (0,76 wt% C) above and blow the eutectoid temperature…….....18
Figure 3.5. Schematic representation of the microstructures for an iron-carbon alloy of hypoeutectoid composition (containing less than 0,76 wt% C) as it is cooled from within the austenite phase region to below the eutectoid temperature……..... 20
Figure 3.6. Photomicrograph of a 0,38 wt% C steel having a microstructure consisting of pearlite and proeutctoid ferrit……..... 21
Figure 3.7. TTT (Time, Temperature, Transformation) curve for a eutectoid steel..... 24
Figure 3.8. Microstructure of tempered martensite……..…...26
Figure 3.9. Thermal path of QTB process…….....28
Figure 3.10. Ferrite “molecule” (body centered cubic)..... 29
Figure 3.11. Martensite “molecule” (hexagonal bipyramid).....30
Figure 3.12. Crude (untempered) martensite..... 30
Figure 3.13. Tempered martensite……..... 31
Figure 3.14. QTB rebar case and core……..……..……...31
Figure 3.15. As-rolled rebar core……..... 32
Figure 3.16. QTB surface, transition and core……..... 32
Figure 3.17. Representation of a functioning QTB cooler ……..…….. 34
Figure 3.18. Representation of QTB coolers in series……..……..34
Figure 3.19. Representation of functioning QTB stripper……..……..……..34

Figure 3.20. Quench depth cross-section…….....37
Figure 3.21. Quench depth longitudinal section……...37
Figure 3.22. Schematic drawing of thermex pipe…….38
Figure 3.23. Magnetic field theories…… 42
Figure 3.24. Picture of used pyrometer……... 44
Figure 3.25. Electromagnetic spectrum……... 45
Figure 4.1. Variation of heat transfer coefficient with surface temperature for ANSI 1025 steel……50
Figure 4.2. Variation of surface temperature with initial liquid temperature for GR60 steel bar …….....52
Figure 4.3. Variation of yield strength with initial liquid temperature for GR60 steel bar….....52
Figure 4.4. Variation of tensile strength with initial liquid temperature for GR60 steel bar…..... ……....53
Figure 4.5. Variation of heat transfer coefficient with surface temperature for ANSI 1025 steeel……...54
Figure 4.6. Variation of surface temperature with relative velocity for GR60 steel bar……...……56
Figure 4.7. Variation of yield strength with relative velocity for GR60 steel bar…… ……..57
Figure 4.8. Variation of tensile strength with relative velocity for GR60 steel bar…….. ……58

LIST OF ABBREVIATIONS AND NOMENCLATURE

ASTM	: American Society for Testing and Materials
Q&P	: Quenching and Partitioning
JIS	: Japanese Rebar Standart
ASZ	: Australiian Rebar Standart
NZS	: New Zelland Rebar Standart
TMT	: Thermo Mechanically Treated
YS	: Yield Strength
UTS	: Ulitamte Tensile Strength
HV	: Hardness Vickers
HK	: Hardness Knoop
HRB	: Rackwell Hardness B scale
HRC	: Rackwell Hardness C scale
QST	: Quenching and Self Tempering
QTB	: Quenched and Tempered Bar
ANN	: Artificial Neural Network
CHF	: Critical Heat Flux
BCC	: Body Centered Cubic
FCC	: Face Centered Cubic
TTT	: Time Temperature Transformation
TME	: Tempered Martensite Embrittlement
TE	: Tempered Embrittlement
CE	: Carbon Equivalent
GR	: Grade
ASIC	: Application Specific Integrated Circuit
PFA	: Perfloro Alkoksi

1. INTRODUCTION

There are many different heat treatment processes for metallic cylindrical materials in industry. Hence, cooling and heating of materials are of great importance. In many applications that use water to cool high temperature surfaces, especially in iron and steel industry, surface heat flux and temperature change rapidly.

Quenching process is used for producing high yield strength concrete-reinforcing steel bars. In quenching process, a bar emerging from last rolling stand is rapidly colled with water and transformation is occurred from austenite to martensite in surface layer. After quenching stage, heat flows from center to surface and self-tempering treatment of martensite is achived. At the same time, austenite core of bar is cooled and transforms generally into ferrite and pearlite. Yield strength and ultimate tensile strength are depended on the percentage of martensite formed.

Quenching of steel in liquid medium consists of four distinct regions of cooling: the film boiling; transition region; nucleate boiling and the forced convective region.

Continuous quenching process consists of three stages. The first stage constitutes fast water-cooling of a hot-rolled product. Effectiveness of the cooling installation should be high enough to achieve the cooling rate of the bar surface higher than the critical speed of martensite formation. At the end of this operation the bar has an austenitic core surrounded by a layer of the martensite-austenite mixture. Obtaining the martensitic layer of the required thickness is the purpose of this stage of the process.

In the second stage the bars leave the water-cooling zone and move towards the air-cooling one. Heat from the hot core propagates in the surface direction causing self-tempering of the martensite layer. The tempering process ensures the proper ductility of material, simultaneously preserving its high yield strength.

The third stage occurs during a free cooling of bars on the cooler and consists of the austenite transformation into ferrite and perlite in the bar core. Successful heat

treatment requires close control over all factors affecting the heating and cooling of a metal.

It can be seen from the literature that investigation of quenching of steel with water, the effects of velocity and subcooling during cooling of steel, the different heat transfer coefficients for boiling regions, surface temperature of steel and water temperature are of great interest.

In this work, 12 mm diameter ASTM A 615/GR60 reinforcing steel was quenched under different initial liquid temperatures and different relative velocities conditions to see variation of material surface temperature, yield strength and ultimate tensile strength. Experiments were performed different season to see effect of temperature difference.

2. LITERATURE REVIEW

Optimal properties of the reinforcing bars are obtained with the application of the Tempcore technology. The process consists of three stages. The first stage constitutes fast water-cooling of a hot-rolled product. Effectiveness of the cooling installation should be high enough to achieve the cooling rate of the bar surface higher than the critical speed of martensite formation. At the end of this operation the bar has an austenitic core surrounded by a layer of the martensite-austenite mixture. Obtaining the martensitic layer of the required thickness is the purpose of this stage of the process. In the second stage the bars leave the water-cooling zone and move towards the air-cooling one. Heat from the hot core propagates in the surface direction causing self-tempering of the martensite layer. The tempering process ensures the proper ductility of material, simultaneously preserving its high yield strength. The third stage occurs during a free cooling of bars on the cooler and consists of the austenite transformation into ferrite and perlite in the bar core. Morphology of structural components depends on the steel chemical composition, bar diameter, time and effectiveness of cooling.

Improvement of strength parameters as well as other metallurgical and mechanical properties of bars rolled in the Tempcore technology allows to decrease reinforcing bars diameters and their total weight - yielding measurable financial savings to investors.

H. Cetinel (2000) and J. Nikolaou (2004) studied designing of the Tempcore technology requires knowledge of the kinetics of phase transformation in plain carbon steels of a low carbon content. Knowledge of the phase transformation kinetics during tempering provides additional possibilities of changes in the heat treatment technology .

Sage AM. (1976), Glodowski RJ. (2000) and Bakkaloglu A. (2002) studied actual methods for the production of high-strength concrete reinforcing steels may be classified into three distinct categories: The first one consists of steel bars slowly cooled in air after hot rolling (hot rolled steels). For these steels, modifying their chemical composition can increase the yield strength, however, for sake of

weldability the carbon and manganese levels should be kept low and this necessarily results in low strength. As an alternative issue, small additions of strong carbide formers, such as Nb andyor V, may enhance the yield strength without affecting weldability.

Rehm G. and Russwurm D. (1977) carried out the solution to 'the hot rolled microalloyed with vanadium or niobium steels', but it is rather expensive, so that use and production of these steels is not widespread. The second category consists of bars submitted to specific thermomechanical strengthening processes, bearing trade-names such as Tempcore, Thermex, etc. The designation 'Tempcore' was adopted since it reflects the principle on which it is based, i.e. tempering of a previously quenched surface layer, under the effect of heat supplied by the core of the bar.

Magallon D. and Huhtiniemi I. (2000) studied the first two corium melt quenching tests in subcooled water performed in the FAT FCI vessel of the FARO facility are described. The tests, referenced as L-29 and L-31, involved 39 and 92 kg of 80 wt% UO2_20 wt% ZrO2 melt, respectively. The molten material was poured into a 1.5-m depth pool of water at 0.2 MPa and ambient temperature. No spontaneous steam explosion occurred. The quenching process was different between the two tests, producing a conglomerate debris bed in L-29 and a particulate debris bed in L-31, with higher thermal load in L-29 than in L-31. The difference in the melt initial temperature is believed to be the cause of this dissimilarity.

Uttara Prasad, Qiang Xu and Mahesh C. Chaturvedi (2002) studied The microstructural evolution in various Ti–45Al based alloys during varying heat treatment conditions. Detailed microstructural investigation of the alloy samples, heated at 1350 °C for 0.5 h and subsequently cooled at different cooling rates, suggested that the alloy's susceptibility to massive transformation increases with increasing the severity of cooling. However, this transformation is quenched by α –> α_2 disorder–order transformation at very high cooling rates (water quenching). It was also observed that cooling rate dependence of transformation modes depends on the composition of the alloy; higher the amount of Mn in the alloy, higher is the cooling rate required for complete massive transformation.

D.V. Edmondsa, K. He, F.C. Rizzo, B.C. De Coomanc, D.K. Matlock and J.G. Speer (2006) described the heat treatment of martensite, different to customary quenching and tempering. This involves quenching to below the martensite-start temperature and directly ageing, either at, or above, the initial quench temperature. If competing reactions, principally carbide precipitation, are suppressed by appropriate alloying, the carbon partitions from the supersaturated martensite phase to the untransformed austenite phase, thereby increasing the stability of the residual austenite upon subsequent cooling to room temperature. This novel treatment has been termed 'quenching and partitioning' (Q&P), to distinguish it from quenching and tempering, and can be used to generate microstructures with martensite/austenite combinations giving attractive properties. Another approach that has been used to produce austenite-containing microstructures is by alloying to suppress carbide precipitation during the formation of bainitic structures, and interesting comparisons can be made between the two approaches. Moreover, formation of carbide-free bainite during the Q&P partitioning treatment may be a reaction competing for carbon, although this could also be used constructively as an additional stage of Q&P partitioning to form part of the final microstructure. Amongst the ferrous alloys examined so far are medium carbon bar steels and low carbon formable TRIP-assisted sheet steels.

Ahmed Ismail Zaky Farahat and S.A. El-Badry (2009) published that although iron and aluminum alloy forms several intermetallic phases, the iron-rich iron aluminide compositions appear to have the most potential for structural applications. A 100 kg of steel containing 0.88 wt.% C, 1.88 wt.% Mn, 0.44 wt.% Si, 0.081 wt.% Cu, 6.9 wt.% Al and 2.00 wt.% Cr was prepared using vacuum induction furnace. The dilatationwas carried out to determine the critical phase transformation. Hot forging process was carried out after heating at 1200 $^{\circ}$C with a high reduction ratio in cross-section 85%. The transformation temperatures A_{c1} and A_{c3} are 897.7 and 964.2 $^{\circ}$C respectively. The density of Fe–Al after hot forging was measured using Archimedes method and it is approximately 6.804gm/cm^3. The as-cast grain size is more than 3000 µm. Hot forging process refines the grain size down to 423 µm. The non-metallic inclusions (after severe hot forging) are very fine andwell

distributed. The material is so sensitive to the final cooling rate after hot forging. After introducing different cooling rates, the material exhibits different tensile characteristics, of sand cooling (slow cooling) the tensile strength is 729.5 MPa and elongation is 3.4%. After air cooling (moderate cooling rate), the strength is 62.1MPa and elongationis 2.9% while of water quenching (drastic cooling), the strength is 559.3 MPa and the elongation is 1.4%.

A.I. Zakya, A. El-Morsyb and T. El-Bitar (2009) studied on effect of different cooling rate with 0.2% C, 0.1% V and 0.02% Nb rebar steel. Billets with 130mm×130mm cross-section were austenitized and hold at 1080 ◦C. The billets were hot rolled to 22mm bar diameter. Hot rolling was finished at 980–1000 ◦C. The final bars were air-cooled. On a parallel way, an experimental hot deformation investigation, on the same steel, was carried out at deformation temperature range 1200–800 ◦C with the same amount of deformation (97% reduction in area). However, cooling regimes after deformation were air cooling, water quenching to 600 ◦C followed by air cooling, and water quenching to room temperature. Microstructure investigation was done using both optical and scanning electron microscopes. Further evaluationwas done using mechanical testing. The industrial trial has unsatisfied results with poorer yield strength with higher ultimate strength. Bainitic aggregates are detected in the hard phases islands. Air cooling after pilot hot deformation creates banded ferrite–pearlite microstructure with 9.11_m ferrite grains. However, quick water quenching to 600 ◦C followed by air cooling develops tempered and softened coarse bainite phase. On the other hand, water quenching to room temperature develops fine bainite texture. Water quenching to 600 ◦C followed by air cooling is the best regime creating accepted mechanical properties.

CSA Standard (1992) published that strength and ductility are critical mechanical properties defined in rebar standards. Primarily, rebar is classified or graded by its yield strength. For instance, the rebar standard in Canada, CSA-G30.18, defines two minimum yield strength levels, 400 and 500 MPa. Japanese Industrial Standard (2005) and Australian/New Zealand Standard (2001) published that many standards also reference a minimum tensile strength level either directly or indirectly. The Japanese rebar standard, JIS G 3112, states a minimum tensile strength level while the

Australian/New Zealand rebar standard, AS/NZS 4671, defines tensile strength indirectly by specifying a minimum strain hardening ratio in reference to the yield strength (i.e. ratio of tensile strength to yield strength).

ASTM standard A 615/A 615M-09 (2009) published that ductility is commonly defined quantitatively by % elongation to fracture or the ratio of tensile to yield strength, and qualitatively by a bendibility test. For example, the US rebar standard, ASTM A 615, requires a minimum percent elongation in an eight inch tensile test sample which varies according to bar diameter and strength level. Similarly, bend tests which specify varying sizes of mandrels and degrees of bend, require that cracks do not form on the bent surface of the bar.

Matthew Allen (2011) studied quench and self-tempering which is another production method used to increase the strength of rebar while limiting the level of carbon and carbon equivalent. In this process, immediately after the rebar exits the final rolling stand in the mill it travels through a series of quenching devices. The particular design of the quenching device is unique to the equipment manufacturer, but in general, high-pressure water is applied against the surface of the bar in order to cool it. In a very short time, this rigorous quenching reduces the surface temperature of the bar to a point where martensite develops. After exiting the quenching area, the remaining heat from the core of the bar conducts outwards and tempers the martensitic surface layer, which helps to increase its ductility. Following this, the bar continues to air-cool until finally the core transforms into a mixture of proeutectoid ferrite and pearlite. Due to the variation in microstructure over the cross-sectional area of the bar, the resulting product can be described as having a composite microstructure. Similar to how reinforced concrete, a composite material, obtains its final properties by a combination and interaction of concrete and steel, quench and self-tempered rebar achieves its beneficial qualities from the combination of the constituent properties of the strong tempered martensite surface and ductile pearlite/ferrite core. Of the three production methods discussed, quench and self-tempering is the most cost effective. It requires a moderate capital investment in new equipment and increase in operating costs; however, it saves on additional labor costs over the off-line work-hardening method and the expensive alloy additions used by the microalloying method. Although this process improves many of the mechanical

properties of the rebar, it unfortunately has a negative effect on the strain-hardening ratio.

B.K. Panigrahi, S. Srikanth, and G. Sahoo (2009) investigated the effect of copper, phosphorus, and chromium present in a semikilled reinforcing bar steel produced by in-line quenching [thermomechanical treatment (TMT)] process on the tensile properties, microstructure, and corrosion resistance of steel in simulated chloride environment. The results have been compared with that of a semikilled C-Mn reinforcing bar steel without these alloying elements produced by the same process route. Though the amount of phosphorus (0.11 wt.%) was higher than that specified by ASTM A 706 standard, the Cu-P-Cr steel exhibited a composite microstructure, and good balance of yield stress, tensile stress, elongation, and ultimate tensile to yield stress ratio. Two conventional test methods, namely, the salt fog, and potentiodynamic polarization tests, were used for the corrosion test. The rust formed on Cu-P-Cr steel was adherent, and was of multiple colors, while the corrosion products formed on the C-Mn steel were weakly adherent and relatively darker blue. Also, the free corrosion potential of the Cu-P-Cr steel was nobler, and the corrosion current was markedly lower than that of a C-Mn rebar. The Cu-P-Cr steel did not develop any pits/deep grooves on its surface even after the prolonged exposure to salt fog. The improved corrosion resistance of the Cu-P-Cr steel has been attributed to the presence of copper, phosphorus, and small amount of chromium in the dense, adherent rust layer on the surface of reinforcing steel bar. A schematic mechanism of charge transfer has been proposed to explain the improved corrosion resistance of the Cu-P-Cr alloyed TMT rebar.

Danieli (2010) developed QTB Plus which is an online system for estimating properties of the Thermo-Mechanically Treated (TMT) bars and wire rods produced in the Bar & Rod Mill and Wire Rod Mill, respectively. The system predicts the Yield strength (YS), Ultimate Tensile Strength (UTS) and Hardness (HV) at different poi,nts across the section of the bar in real time during actual processing. The Mill Automation System captures data from the Quenching and Self-Tempering (QST) process through field devices. The QTB Plus Model suite then calculates the thermal histories of different annual segments of the bar. Finally, the system uses these histories to estimate the final

microstructure of these individual segments. This is done with the help of a series of models – Thermal Model, Microstructural Model, Phase Transformation Model and Property Model. The final property of rebar, so obtained, id generally substantiated with the help of an additional Artificial Neural Network (ANN) model to account for the uncertainties of the actual processing in the plant. Apart from predicting properties of plain bars, rebars and wire rods, Danieli QTB Plus System is useful to produce desired mechanical properties through proper process control. For any given final strength of the bar, the system calculate set-up parameters of the Quenching Process. Thus, the system predicts and controls mechanical properties of the bars in real time. The assessment of properties helps proper monitoring and thereby ensures. Prediction of properties helps reduce the sampling size of mechanical testing. The system can be used to design new grades of bar with superior quality, such as improved weldability, elongation and bendability. It helps performe process optimization and parameter design.

Yılmaz et. al. (2005) investigated the influence of variable physical properties of ANSI 1025 and AISI 304 steels and different boundary conditions namely forced convection, free convection and radiation on the calculation of cooling process. They solved numerically the governing differential equations for nonsteady cases.

Forced convection film boiling heat transfer coefficients on a 3 mm diameter vertical cylinder were obtained for the flow velocities ranging from 0 to 3 m/s and pressures from 102 to 490 kPa under saturated condition in water and for the liquid subcoolings ranging from 0 to 60 ^{o}C in R113 by Shiotsu and Hama (2000). They derived the correlation for the forced convection film boiling heat transfer with radiation contribution on a vertical cylinder by modifying an approximate analytical solution for a two-phase laminar boundary layer model to agree better with the experimental data. They found that the heat transfer coefficients for each liquid subcooling and flow velocity are higher for higher pressure.

Liu et. al. (1992) measured the forced convection film boiling heat transfer from a horizontal cylinder in water or R113 flowing upward perpendicular to the cylinder under saturated condition for the flow rates ranging from 0 to 1 m/s at the system pressures ranging from 100 to 500 kPa. They used platinum cylinders with the diameters ranging from 0.7 to 5 mm as the test heaters. They plotted the

variations of film boiling heat transfer coefficients versus cylinder surface superheats for 3 mm diameter cylinder in water and in R113, respectively, with flow rate as a parameter. They also plotted the variations of the heat transfer coefficients versus flow rates with the cylinder diameter as a parameter. They found that the film boiling heat transfer coefficients were weakly dependent on the cylinder surface superheat but significantly dependent on flow rate, system pressure and cylinder diameter; the heat transfer coefficients were higher for higher flow rate, higher system pressure and smaller cylinder diameter. They suggested a new forced convection film boiling heat transfer correlation by modifying an approximate analytical solution for a laminar flow film boiling model derived by the authors to comply with the experimental data.

Heat transfer was calculated for a cylinder similar to a jominy experiment specimen by Chen et. al. (1999). They carried out experimental work using AISI 1015 steel. They determined surface heat flux both experimentally and numerically, however, they assumed constant physical properties during numerical calculations. They aimed to calculate the heat flux and temperature distribution of the quenching surface, where the temperatures were not easy to measure during quenching. They found that the predicted surface temperature and heat flux of the end quenching problem were acceptable by experimental verification.

Hammad et. al. (2004) carried out an experimental work to study the characteristics of heat transfer and wetting front during quenching high temperature cylindrical block by water jet at atmospheric pressure. They calculated the surface temperature and heat flux by applying a two-dimensional inverse solution which makes it possible successfully estimate surface temperature and heat flux from the measured temperatures in the solid. They used a high speed video camera to observe the movements of both wetting front and transition boiling region over the heated block surface. They investigated different conditions, liquid subcooling ΔT_{sub} of 5, 20, 50 and 80 ^{o}C and jet velocity of 3, 5, 10 and 15 m/s in the experiments. They found that the time that was needed to start the maximum heat flux over the heated surface was longer at a condition of low subcooling and low jet velocity than at a condition of high subcooling and high jet velocity.

In another work, Mozumder et. al. (2006) conducted an experimental investigation for quenching of hot cylindrical blocks made of copper, brass and steel by a subcooled water jet of diameter of 2 mm. They proposed a new correlation for maximum heat flux. The maximum heat flux is a strong function of the position on the hot surface, jet velocity, block material properties and jet subcooling. They presented the variation of maximum heat flux with jet velocity and subcooling. The subcooling was 5 to 80 ^{o}C and the jet velocity was 3 to 15 m/s. They found that the maximum heat flux increases gradually with increasing jet velocity and higher subcooling increases the thermal potential between the solid and the impingent liquid which results in higher q_{max}.

Chen et. al. (2004) performed an experimental study of single-bubble subcooled boiling heat transfer ($\Delta T_{sub} = 31.5$ ^{o}C) on a small heater with constant wall temperature to examine the associated complex heat transfer process. They used in their experiment FC-72 as the boiling fluid which was widely used in electronics cooling. The bulk fluid was maintained at ambient conditions (1 atm and 24.5 ^{o}C), and its corresponding saturation temperature was 56 ^{o}C for all the experiments performed.

Hua and Xu (2000) investigated the quenching boiling of small spheres and a circular plate into saturated and subcooled liquid nitrogen. Effects of the diameters of spheres and the subcooling of liquid nitrogen on quenching boiling were investigated. They found that subcooling increased the heat transfer of liquid nitrogen on small samples. When a sphere with a diameter of 0.3 mm was quenched into the liquid nitrogen with subcooling of 11.9 ^{o}C, the maximum heat flux was obtained as three times higher than that in saturated case. They also found that subcooling of liquid nitrogen increased the heat fluxes on large plate surface up to 80% higher than in saturated case.

Yang et. al. (2006) conducted an experimental study to investigate the viability of using an appropriate vessel coating to enhance the critical heat flux (CHF) limits during external reactor vessel cooling. They performed the transient quenching and steady-state boiling experiments in the boundary layer boiling and obtained local boiling curves and CHF limits in these experiments.

Abou-Ziyan (2004) carried out an experimental work to investigate the heat transfer from the heated bottom side of T cross-section ducts to an internally flowing fluid. He aimed to provide better design information for the cooling of critical areas in the cylinder heads of internal combustion engines. He reported fully developed single phase forced convection and subcooled flow boiling heat transfer data. Six T-ducts of different width and height aspect ratios were tested with distilled water at velocities of 1, 2 and 3 m/s for bulk temperatures of 60 and 80 ^{o}C. He found that the heat transfer coefficients for flow velocities of 2 and 3 m/s were higher than those for 1 m/s by about 60 % and 140 %, respectively, and the boiling heat fluxes were increased in average by about 62-98 % as the water velocity increased from 1 to 2 m/s. He also found that the increase in the fluid bulk temperature deteriorated the boiling heat flux. He developed a correlation for Nusselt number as a function of Reynolds number, Prandtl number, viscosity ratio and some aspect ratios of the T-duct.

3. MATERIAL AND METHOD

Steels can be heat treated to produce a great variety of microstructures and properties. Generally, heat treatment uses phase transformation during heating and cooling to change a microstructure in a solid state.

In heat treatment, the processing is most often entirely thermal and modifies only structure. Thermomechanical treatments, which modify component shape and structure, and thermochemical treatments which modify surface chemistry and structure, are also important processing approaches which fall into the domain of heat treatment.

3.1. Quenching Process

Several terms used in iron-carbon (Fe-C) alloys: Ferrite (α-iron), Austenite (γ-iron), Cementite (iron carbide, Fe3C), Pearlite (88wt% ferrite, 12wt% cementite, or 99.2wt% iron, 0.8wt% carbon), Bainite, Martensite, Ledeburite (ferrite-cementite eutectic, 4.3% carbon).

Ferrite: the α-iron, is a materials science term for iron, or a solid solution with iron as the main constituent, with a body centered cubic (bcc) crystal structure. It is the component which gives steel and cast iron their magnetic properties, and is the classic example of a 2 ferromagnetic material. Practically speaking, ferrite can be considered pure iron. Ferrite is stable below 910 °C (1,670 °F). Above this temperature the face centered cubic (fcc) form of iron, austenite (γ-iron), is stable. Above 1,390 °C (2,530 °F), up to the melting point at 1,539 °C (2,802 °F), the body centered cubic (bcc) crystal structure is again the more stable form for delta-ferrite (δ-Fe). Only a very small amount of carbon can be dissolved in ferrite; the maximum solubility is about 0.02 wt% at 723 °C (1,333 °F) and 0.005% carbon at 0 °C (32 °F). This is because carbon dissolves in iron interstitially, with the carbon atoms being about twice the diameter of the interstitial "holes", so that each carbon atom is surrounded by a strong local strain field. Hence the enthalpy of mixing is positive

(unfavourable), but the contribution of entropy to the free energy of solution stabilizes the structure for low carbon content.

Pearlite: is a two-phased, lamellar (or layered) structure composed of alternating layers of ferrite (88 wt%) and cementite (12wt%) that occurs in some steels and cast irons. During slow cooling pearlite forms by a eutectoid reaction as austenite is cooled below 727°C (the eutectoid temperature). Mild steel (carbon steel with up to about 0.2 wt% C) consist mostly of ferrite, where the amount of pearlite increases with increasing the carbon content is increased.

Austenite: the γ-iron, is a metallic non-magnetic allotrope of iron or a solid solution of iron, with an alloying element (typically carbon). In plain-carbon steel, austenite exists above the critical eutectoid temperature of 727 °C); other alloys of steel have different eutectoid temperatures. It is named after Sir William Chandler Roberts-Austen (1843-1902)

Cementite: iron carbide (Fe3C), is a chemical compound of an orthorhombic crystal structure. It is a hard, brittle material, normally classified as a ceramic in its pure form, though it is more important in metallurgy. Cementite forms directly from the melt in the case of white cast iron. In carbon steel, it either forms from austenite during cooling or from martensite during tempering. An intimate mixture with ferrite, the other product of austenite, forms a lamellar structure called pearlite. Much larger lamellae, visible to the naked eye, make up the structure of Damascus steel.

Martensite: named after the German metallurgist Adolf Martens (1850–1914), most commonly refers to a very hard form of steel crystalline structure, but it can also refer to any crystal structure that is formed by displacive transformation. Martensite is not shown in the equilibrium phase diagram of the iron-carbon system because it is a metastable phase, the kinetic product of rapid cooling of steel containing sufficient carbon.

Bainite: first described by E. S. Davenport and Edgar Bain, is a phase that exists in steel microstructures after certain heat treatments. Bainite is one of the decomposition products that may form when austenite is cooled past the eutectoid temperature of 727 °C. appearing as a fine non-lamellar structure, bainite commonly consists of ferrite, carbide, and retained austenite. In these cases it is similar in

constitution to pearlite, but with the ferrite forming by a displacive mechanism similar to martensite formation, usually followed by precipitation of carbides from the supersaturated ferrite or austenite. The temperature range for transformation to bainite is between those for pearlite and martensite. When 3 formed during continuous cooling, the cooling rate to form bainite is higher than that required to form pearlite, but lower than that to form martensite, in steel of the same composition.

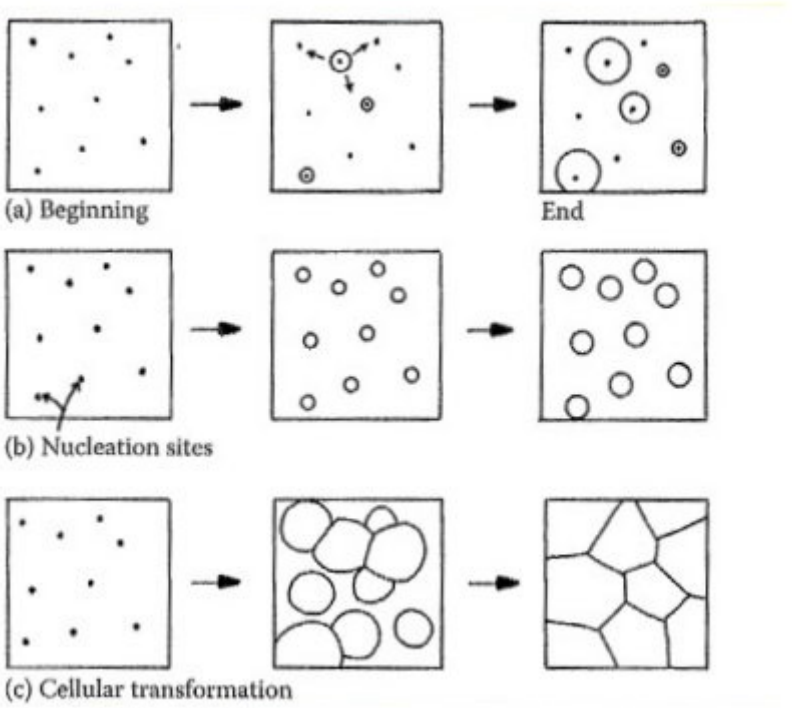


Figure 3.1. (a) Nucleation at a constant rate during the whole transformation. (b) Site saturation-all nucleation occurs at the beginning of transformation. (c) Cellular transformation.

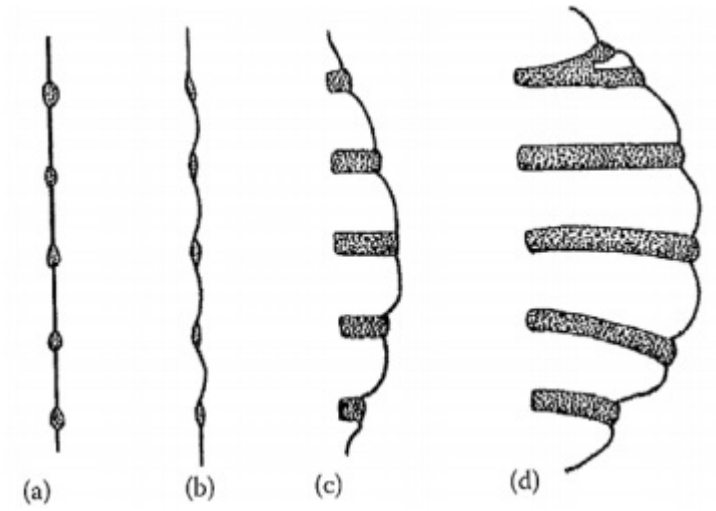


Figure 3.2. Schematic diagram showing a possible sequence of step during the development of cellular precipitation.

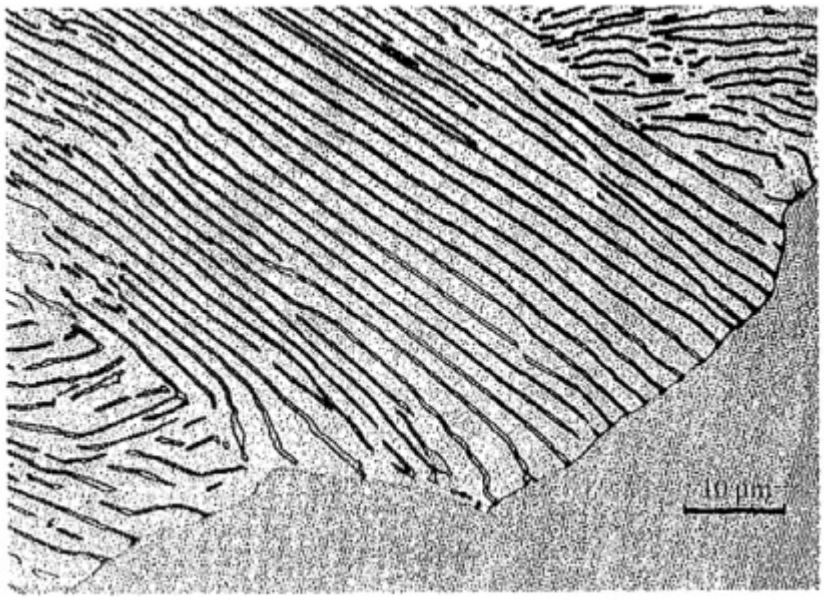


Figure 3.3. Pearlite colony advancing into an austenite grain.

A eutectic system is a mixture of chemical compounds or elements that has a single chemical composition that solidifies at a lower temperature than any other composition. This composition is known as the eutectic composition and the temperature is known as the eutectic temperature. On a phase diagram the intersection of the eutectic temperature and the eutectic composition gives the eutectic point.

$$\text{Liquid} \xrightarrow[\text{cooling}]{\text{eutectic temperature}} \alpha \text{ solid solution} + \beta \text{ solid solution}$$

The eutectic transformation is usually defined as: This type of transformation is an invariant reaction, because it is in thermal equilibrium, i.e., the Gibbs free energy change equals zero. This means the liquid and two solid solutions all coexist at the same time and are in chemical equilibrium.

When the solution above the transformation point is solid, rather than liquid, an analogous eutectoid transformation can occur. For instance, in the iron-carbon (Fe-C) system, the austenite phase can undergo a eutectoid transformation to produce ferrite and 5 cementite, often in lamellar structures such as pearlite. This eutectoid point occurs at 727 °C (1,341 °F).

The eutectoid composition of austenite is approximately 0.8% carbon; steel with less carbon content will contain a corresponding proportion of relatively pure ferrite crystallites that do not participate in the eutectoid reaction and cannot transform into pearlite. Likewise steels with higher carbon contents will form cementite before reaching the eutectoid point.

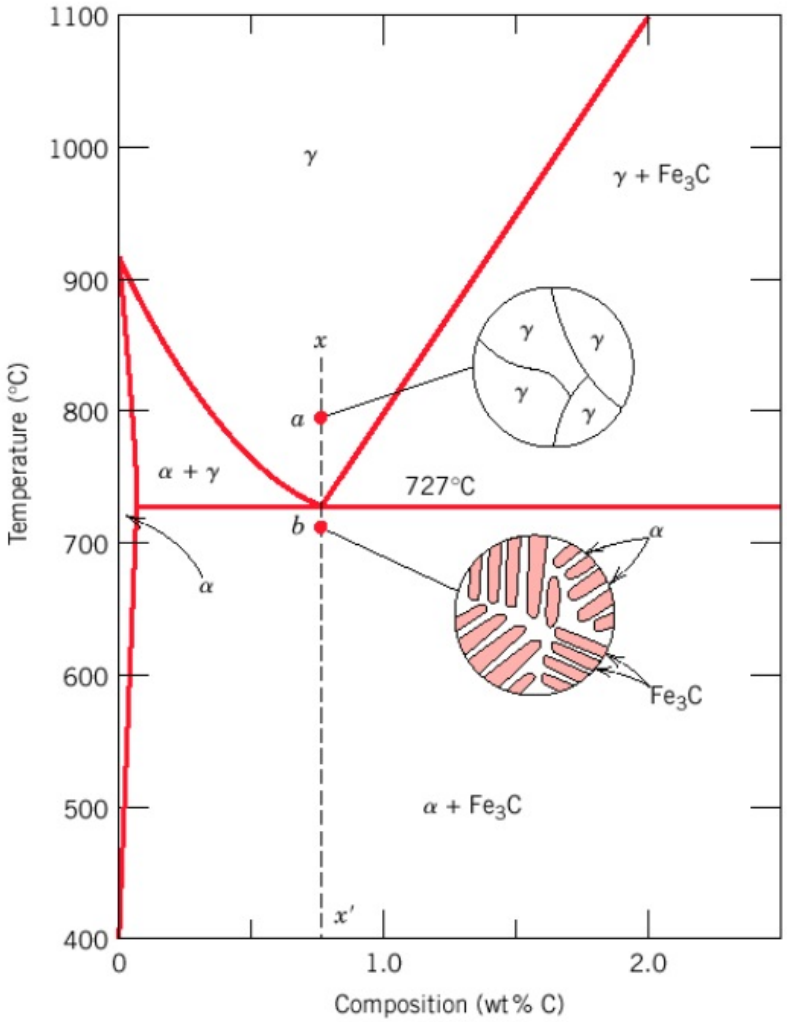


Figure 3.4. Schematic representation of the microstructures for an iron-carbon alloy of eutectoid composition (0,76 wt% C) above and blow the eutectoid temperature.

A eutectoid alloy is similar in behavior to a eutectic alloy. An eutectic alloy is characterized by having a single melting point. This melting point is lower than that of any of the constituents, and no change in the mixture will lower the melting point any further. When a molten eutectic alloy is cooled, all of the constituents will crystallize into their respective phases at the same temperature.

A eutectoid alloy is similar, but the phase change occurs, not from a liquid, but from a solid solution. Upon cooling a eutectoid alloy from the solution temperature, the constituents will separate into different crystal phases, forming a single microstructure. A eutectoid steel, for example, contains 0.77% carbon. Upon

cooling slowly, the solution of iron and carbon, (a single phase called austenite), will separate into platelets of the phases ferrite and cementite. This forms a layered microstructure called pearlite. See Figure 3.3 and Figure 3.4.

Since pearlite is harder than iron, the degree of softness achieveable is typically limited to that produced by the pearlite. Similarly, the hardenability is limited by the continuous martensitic microstructure formed when cooled very fast.

Eutectoid steel can in principle be transformed completely into pearlite;hypoeutectoid steels can also be completely pearlitic if transformed at a temperature below the normal eutectoid. Pearlite can be hard and strong but is not particularly tough. It can be wear resistant because of a strong lamellar network of ferrite and cementite. Examples of applications include cutting tools, high strength wires, knives, chisels, and nails.

If a sample of 0.4% C, hypoeutectoid steel is heated to about 900°C (point c) for a sufficient time, its structure will become homogenous austenite. Then if is slowly cooled to temperature at point d, proeutectoid ferrite will nucleate and grow at the austenite grain boundaries. If this alloy is slowly cooled from temperature at point d to point e, the amount of proeutectoid ferrite formed will continue to increase until about 50% of the austenite is transformed. While the steel is cooling from point d to point e, the carbon content of the remaining austenite will be increased from 0.4% to 0.8%. At 727°C, the remaining austenite will transform isothermally into pearlite according to the eutectoid reaction. The α ferrite in the pearlite is called eutectoid ferrite to distinguish it from the proeutectoid ferrite. This transformation and micro structure is shown in Figure 3.5 and Figure 3.6.

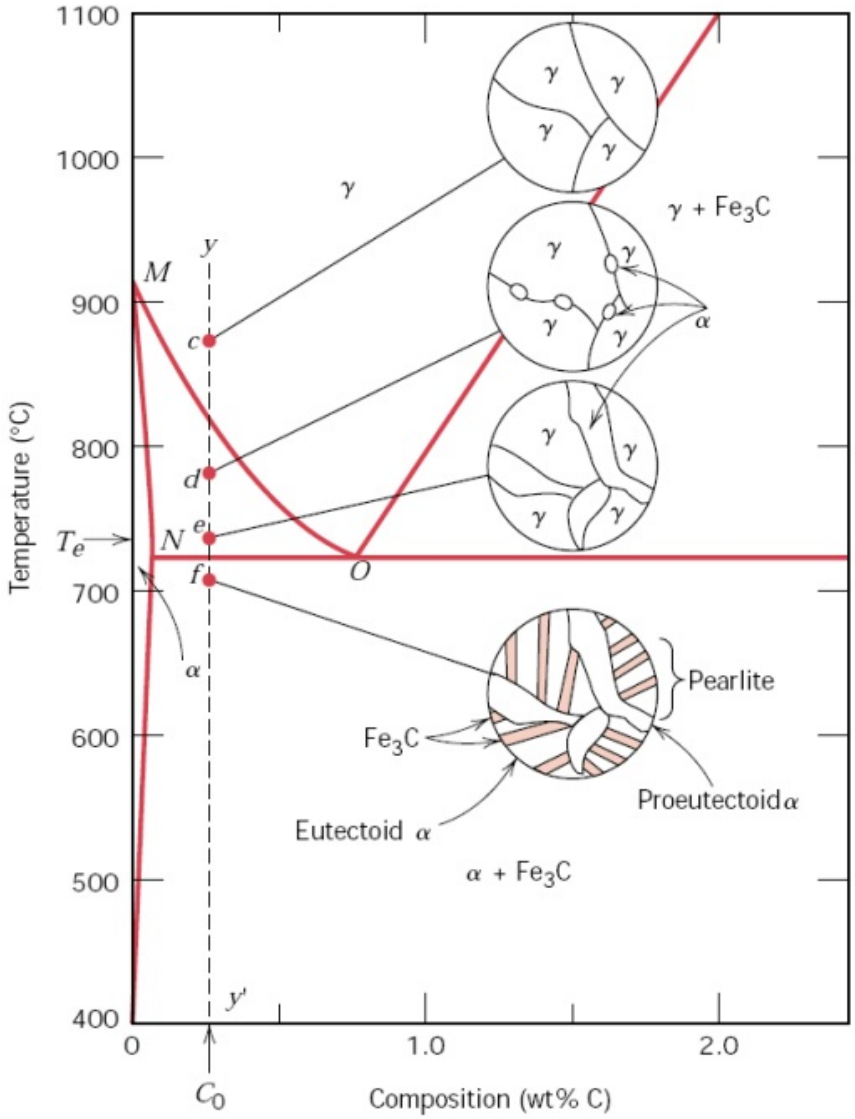


Figure 3.5. Schematic representation of the microstructures for an iron-carbon alloy of hypoeutectoid composition (containing less than 0,76 wt% C) as it is cooled from within the austenite phase region to below the eutectoid temperature.

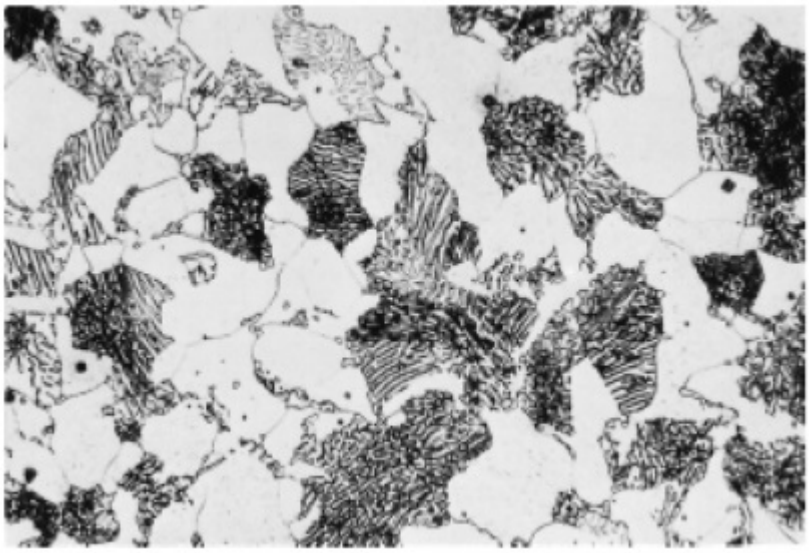


Figure 3.6. Photomicrograph of a 0,38 wt% C steel having a microstructure consisting of pearlite and proeutctoid ferrit.

The various types of heat-treating processes are similar because they all involve the heating and cooling of metals; they differ in the heating temperatures and the cooling rates used and the final results. The usual methods of heat-treating ferrous metals (metals with iron) are annealing, normalizing, hardening, and tempering. Most nonferrous metals can be annealed, but never tempered, normalized, or case-hardened.

The cooling rate of an object depends on many things. The size, composition, and initial temperature of the part and final properties are the deciding factors in selecting the quenching medium. A quenching medium must cool the metal at a rate rapid enough to produce the desired results.

Mass affects quenching in that as the mass increases, the time required for complete cooling also increases. Even though parts are the same size, those containing holes or recesses cool more rapidly than solid objects. The composition of the metal determines the maximum cooling rate possible without the danger of cracking or warping. This critical cooling rate, in turn, influences the choice of the quenching medium.

The cooling rate of any quenching medium varies with its temperature; therefore, to get uniform results, you must keep the temperature within prescribed

limits. The absorption of heat by the quenching medium also depends, to a large extent, on the circulation of the quenching medium or the movement of the part. Agitation of the liquid or the part breaks up the gas that forms an insulating blanket between the part and the liquid.

Normally, hardening takes place when you quench a metal. The composition of the metal usually determines the type of quench to use to produce the desired hardness. For example, shallow-hardened low-alloy and carbon steels require severer quenching than deep-hardened alloy steels that contain large quantities of nickel, manganese, or other elements. Therefore, shallow-hardening steels are usually quenched in water or brine, and the deep-hardening steels are quenched in oil. Sometimes it is necessary to use a combination quench, starting with brine or water and finishing with oil. In addition to producing the desired hardness, the quench must keep cracking, warping, and soft spots to a minimum.

The volume of quenching liquid should be large enough to absorb all the heat during a normal quenching operation without the use of additional cooling. As more metals are quenched, the liquid absorbs the heat and this temperature rise causes a decrease in the cooling rate. Since quenching liquids must be maintained within definite temperature ranges, mechanical means are used to keep the temperature at prescribed levels during continuous operations.

The critical temperatures (A1, A6, and Acm) are “arrests” in heating or cooling and have been symbolized with the letter A, from the French word arret meaning arrest or a delay point, in curves plotted to show heating or cooling of samples. Such changes occur at transformation temperatures in the iron-cementite diagram if sufficient time is given and cab be plotted for steels showing lags at transformation temperature. However, because heating rates in commercial practice usually exceed those in controlled laboratory experiments, changes on heating usually occur at temperatures a few degrees above and are known as Ac temperatures, such as Ac1 or Ac3. The “c” is from the French ,word chauffage, meaning heating. Thus, Ac1 is a few degrees above the ideal A1 temperature. Likewise, on slow cooling in commercial practice, transformation changes occur at temperatures a few degrees. These are known as Ar, or Ar3, the “r” originating from

the French word refroidissement, meaning cooling. This difference between the heating and cooling varies with the rate of heating or cooling. The faster the heating, the higher the Ac point; the faster the cooling , the lower the Ar point. Also, the faster the heating and cooling rate, the greater the gap between the Ac and Ar points of the reversible (equilibrium) point A. Going one step further, in cooling a piece of steel, it is of utmost importance to note that the cooling rate may be so rapid (as in quenching steel in water) as to suppress the transformation for several hundreds of degrees. This is due to the decrease in reaction rate with decrease in temperature. As discussed subsequently, time is an important factor in transformation, especially in cooling.

The foregoing discussion has been confined principally to phases that are formed by various combinations of composition and temperature; little reference has been made to the effects of time. In order to convey to the reader the effects of time on transformation, the simplest approach is by means of a time-temperature-transformation (TTT) curve for some constant iron-carbon composition. TTT curves are also known as “S” curves because the principal part of the curve is shaped like the letter “S.”. TTT curve for eutectoid steel is shown in Figure 3.7. Temperature is plotted on the vertical axis, and time is plotted on a logarithmic scale along the horizontal axis. The reason for plotting time on a logarithmic scale is merely to keep the width of the chart within a manageable dimension. Begin with line Ae1 (725 C or 1340 F). Above this temperature, austenite exists only for a eutectoid steel. When the steel is cooled and held at a temperature just below Ae1 (705 C or 1300 F), transformation begins (follow line (Ps Bs), but very slowly at this temperature; 1 h of cooling is required before any significant amount of transformation occurs, although eventually complete transformation occurs isothermally (meaning at a constant temperature), and the transformation product is spheroidite. Now assume a lower temperature (650 C or 1200 F) on line Ps Bs (the line of beginning transformation); transformation begins in less than 1 min, and the transformation product is coarse pearlite. Next, assume a temperature of 540 C (1000 F); transformation begins in approximately 1 s and is completely transformed to fine pearlite in a matter of a few minutes. The line Pf Bf represents the completion of transformation and is generally

parallel with Ps Bs. However, if the steel is cooled very rapidly (such as by immersing in water) so that there is not sufficient time for transformation to begin in the 540 C (1000 F) temperature vicinity, then the beginning of transformation time is substantially extended. For example, if the steel is cooled to and held at 315 C (600 F), transformation does not begin for well over 1 min. It must be remembered that all of the white area to the left of line Ps Bs represents the austentic phase, although it is highly unstable. When transformation takes place isothermally within the temperature range of approximately 290 to 425 C (550 to 800 F), the transformation product is a microstructure called bainite. In another example, steel is cooled so rapidly that no transformation takes place in the 540 C (1000 F) region and rapid cooling is continued to and below 275 C (530 F) or Ms. Under these conditions, martensite is formed. Point Ms is the temperature at which martensite begins to form, and Mf indicates the complete finish of transformation. It must be remembered that martensite is not a phase but is a specific microstructure in the ferritic (alpha) phase. Martensite is formed from the carbon atoms jamming the lattice of the austenitic atomic arrangement. Thus, martensite can be considered as an aggregate of iron and cementite.

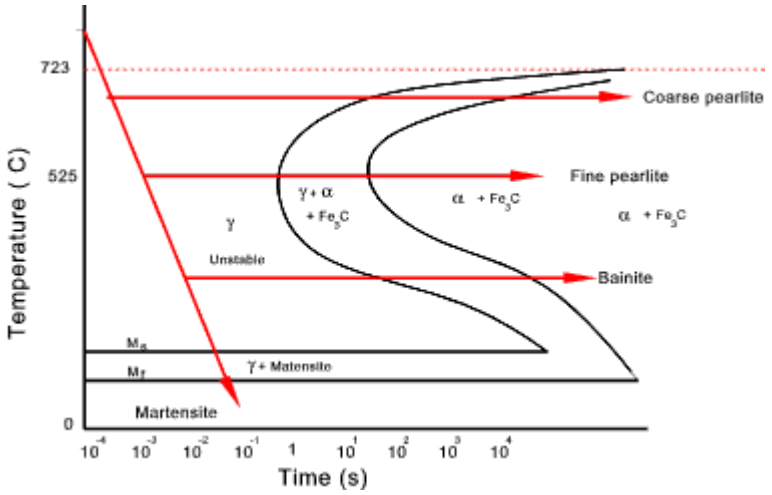


Figure 3.7. TTT (Time, Temperature, Transformation) curve for a eutectoid steel.

Tempering is most often performed on steel that has been heated above its upper critical (A3) temperature and then quickly cooled, in a process called

quenching, using methods such as immersing the red-hot steel in water, oil, or forced-air. The quenched-steel, being placed in, or very near, its hardest possible state, is then tempered to incrementally decrease the hardness to a point more suitable for the desired application. The hardness of the quenched-steel depends on both cooling speed and on the composition of the alloy. Steel with a high carbon-content will reach a much harder state than steel with a low carbon-content. Likewise, tempering high-carbon steel to a certain temperature will produce steel that is considerably harder than low-carbon steel that is tempered at the same temperature. The amount of time held at the tempering temperature also has an effect. Tempering at a slightly elevated temperature for a shorter time may produce the same effect as tempering at a lower temperature for a longer time. Tempering times vary, depending on the carbon content, size, and desired application of the steel, but typically range from a few minutes to a few hours.

Tempering quenched-steel at very low temperatures, between 66 and 148 °C (151 and 298 °F), will usually not have much effect other than a slight relief of some of the internal stresses. Tempering at higher temperatures, from 148 to 205 °C (298 to 401 °F), will produce a slight reduction in hardness, but will primarily relieve much of the internal stresses. Tempering in the range of 260 and 340 °C (500 and 644 °F) causes a decrease in ductility and an increase in brittleness, and is referred to as the "tempered martensite embrittlement" (TME) range. Except in the case of blacksmithing, this range is usually avoided. Steel requiring more strength than toughness, such as tools, are usually not tempered above 205 °C (401 °F). Instead, a variation in hardness is usually produced by varying only the tempering time. When increased toughness is desired at the expense of strength, higher tempering temperatures, from 370 to 540 °C (698 to 1,004 °F), are used. Tempering at even higher temperatures, between 540 and 600 °C (1,004 and 1,112 °F), will produce excellent toughness, but at a serious reduction in the strength and hardness. At 600 °C (1,112 °F), the steel may experience another stage of embrittlement, called "temper embrittlement" (TE), which occurs if the steel is held within the TE temperature range for too long. When heating above this temperature, the steel will

usually not be held for any amount of time, and quickly cooled to avoid temper embrittlement.

When martensite is tempered, it partially decomposes into ferrite and cementite. Tempered martensite is not as hard as just-quenched martensite, but it is much tougher. Micro structure of temperet martensite is shown in Figure 3.8. Note also that it is much finer-grained than just-quenched martensite.

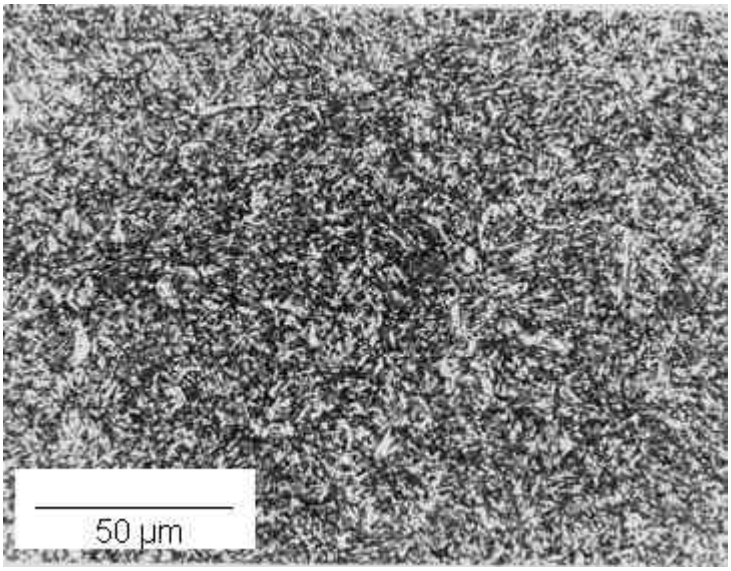


Figure 3.8. Microstructure of tempered martensite.

3.1.1 Continuous Quenching

Strengthening in steel is generally achieved by adding alloys to the liquid steel, causing distortions of the molecular lattice. Some of the steel standards that are available are either very open on the chemistry requirements or else have no chemical restrictions at all. Two examples of such a standard are A615 and A706 for rebar production.

The continuous quenching process utilizes quenching and self-tempering technology during the final stages of rolling, whereas the ordinary rolling process does not. The rebars produced by the continuous quenching process are known as quenched and self tempered rebars or QST rebars.

Jacob Selzer (2012) described QTB is designed to be installed in-line with the rolling process. The hot rolled bar is fully submerged in water in order to rapidly cool the surface of the bar below the martensitic transformation temperature. This phase of the process creates a hardened "case" on the outside of the bar. The core of the bar remains austenitic. The residual heat in the core of the bar radiates out to the shell of the bar, tempering the newly formed martensite. During this time, the surface of the bar reheats to approximately 600-700°C. After the bar reaches its peak reheat temperature, it cools naturally until reaching ambient temperatures. Figure 3.9 shows the typical cooling and reheating curves of the surface of the bar, the center of the bar and the midway point of the bar. The figure also shows the microstructure before quenching, after quenching and after tempering. The final bar has a pearlite core, a thin layer of mixed bainite and an outer shell of tempered martensite.

After the bar has reached ambient temperature, it behaves more like a composite material than a single, solid material. For example, steel-reinforced concrete has the tension-bearing properties of the steel and the compression strength of the concrete. Similarly, a QTB bar has the ductility of the core of the bar and the strength of the case of the bar. By reducing the alloy additions, the core of the bar is softer and more ductile than the fully alloyed counterpart. The tensile strength is determined by the combination of bar chemistry and the depth of quench achieved during the quenching phase of the process. The end result is that the elongation penalty is reduced when increasing yield and tensile strength, compared to traditional strengthening methods for hot rolled bar.

Steel that is manufactured from recycled scrap can face another challenge related to the raw materials. There are elements that can have significant impact to the mechanical properties of the steel that are present in ever-changing quantities in the scrap and in the final product. Examples of these elements are Cr, Ni, Mo, Co and W. The aim carbon for a typical QTB rebar application is between 0.25 and 0.30%. As a result, carbide-forming residuals have a lessened effect compared to when they are found in fully alloyed steel. Also, when using QTB, the mechanical properties are not determined by chemistry alone, so the operator is able to adjust the quenching phase of the process to adapt to the changes in chemistry. The process is

able to absorb a wider range of residuals in the steel scrap compared to a more traditional process, while still achieving the strength aims of the standard being manufactured.

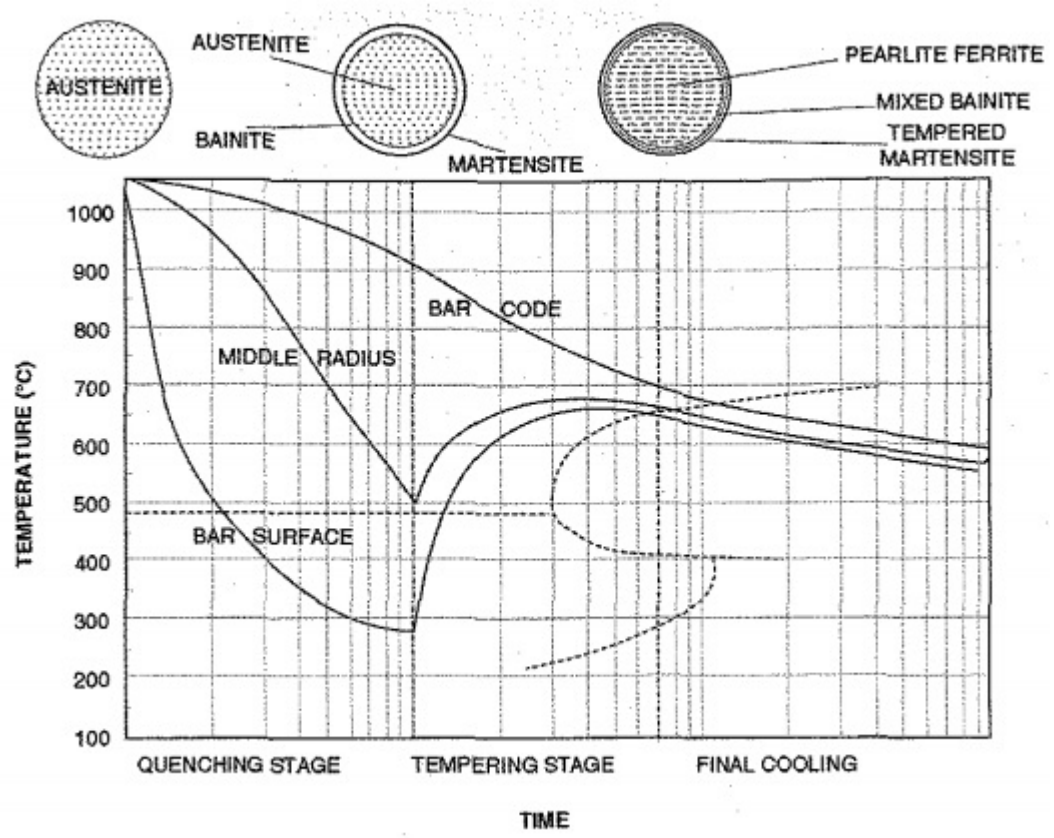


Figure 3.9. Thermal path of QTB process.

Steel is an allotropie material, meaning it can exist in different crystalline structures. Most "plain" carbon steel exists in the ferrite microstructure. It is magnetic, stable and, for the strength it imparts, it remains reasonably ductile. Because steel is allotropie, it can be heat treated to change the mechanical properties of the metal. An alternate steel microstructure that is also stable at ambient temperature is martensite. Martensite is stronger and harder than ferrite and has a correspondingly lower ductility. Figures 3.10 and 3.11 represent comparison renderings of the molecular structures. The ferrite rendering (Figure 3.10) is typical of most carbon steels. The martensite rendering (Figure 3.11) is typical of the surface (case) of a QTB-treated bar. Tempering the martensite is necessary to reduce internal

stresses to the newly formed martensite and to eliminate brittleness in the final bar. Comparison micro etches are shown in Figures 3.12 and 3.13. The core of the QTB-treated bar (Figure 3.14) is pearlitic. Grain refinement of the pearlitic core of the bar is observed compared with as-rolled bar of identical chemistry (Figure 3.15). This grain refinement contributes to the generally improved elongations of QTB-treated bar compared to the fully alloyed bar. This characteristic of the QTB-treated bar allows the manufacturer to increase the strength of the bar without sacrificing ductility of the bar. Figure 3.16 is a micro etch of a QTB-treated bar showing the surface and the microstructural transition from surface to core. This sample is 3/4 inch, grade 60 rebar with chemistry conforming to AISI 1026. Starting at the surface of the bar, the microstructure is tempered martensite. Moving toward the center of the bar, the tempering becomes more pronounced, which is viewed as a "softening" of the microstructure. At the transition from martensite to ferrite, approximately 0.035 inch below the surface, there is some evidence of mixed bainite. The pearlitic structure begins from this point through to the center of the bar.

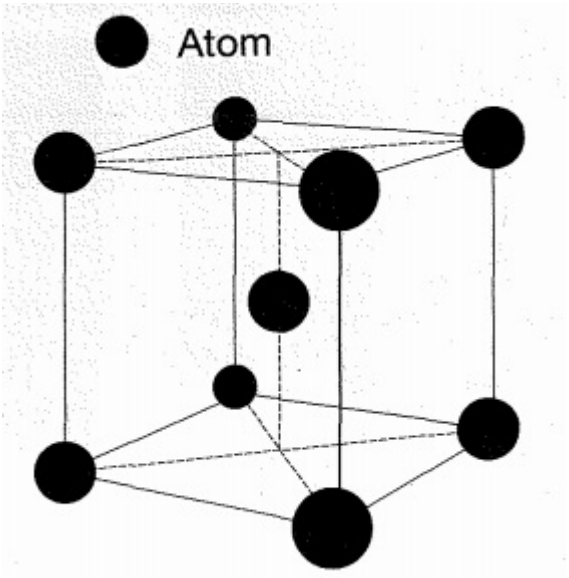


Figure 3.10. Ferrite “molecule” (body centered cubic).

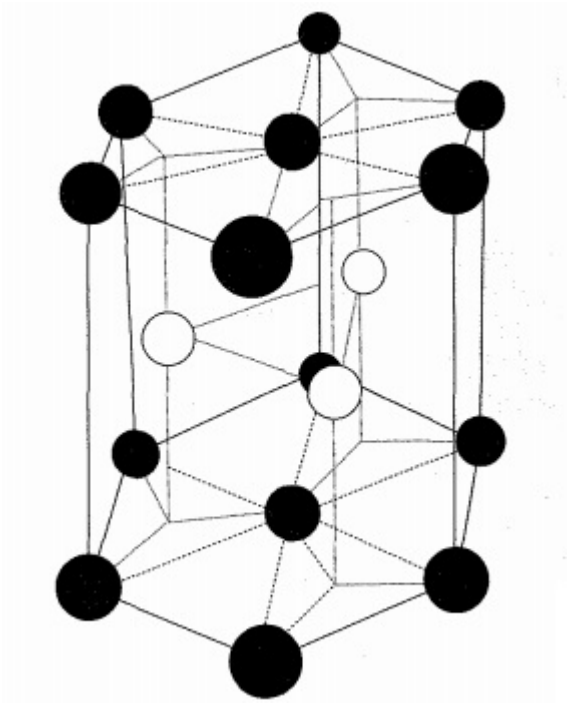


Figure 3.11. Martensite “molecule” (hexagonal bipyramid).

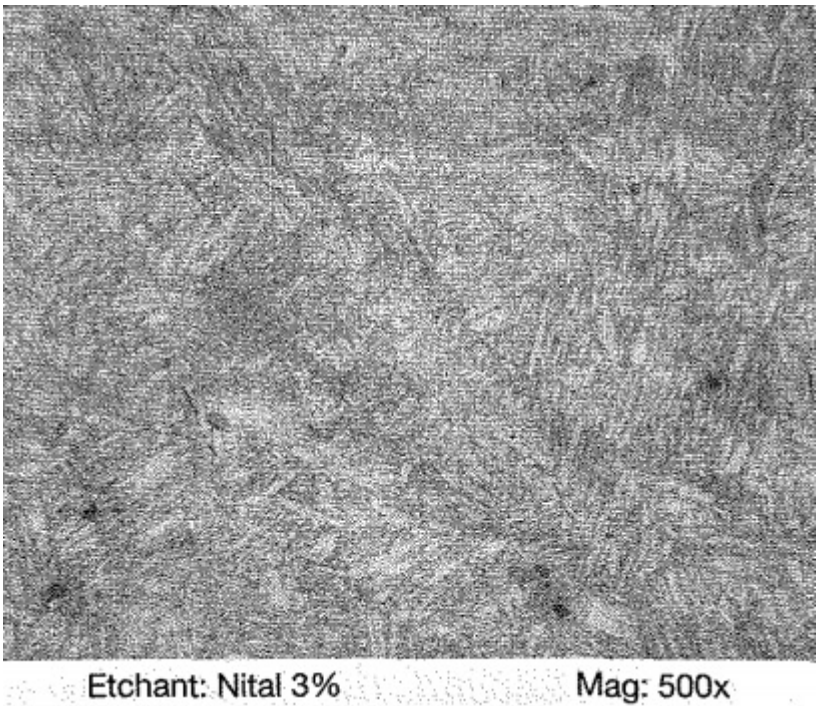


Figure 3.12. Crude (untempered) martensite.

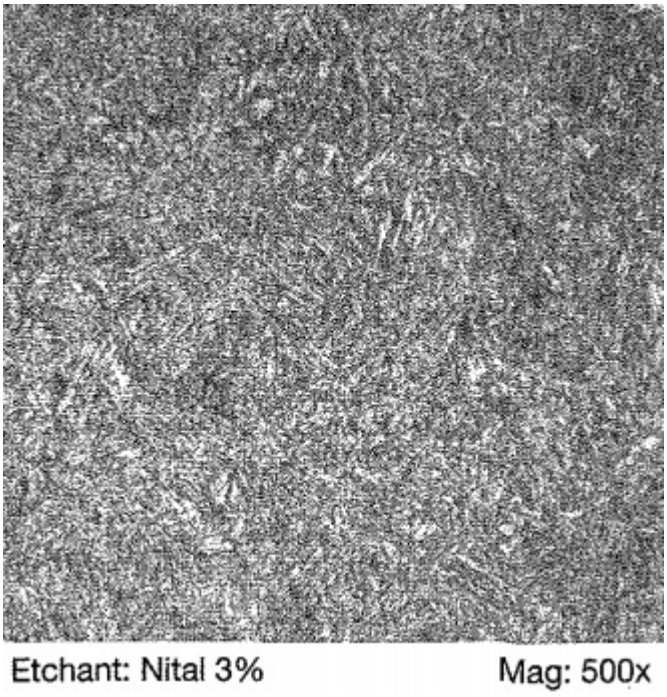


Figure 3.13. Tempered martensite.

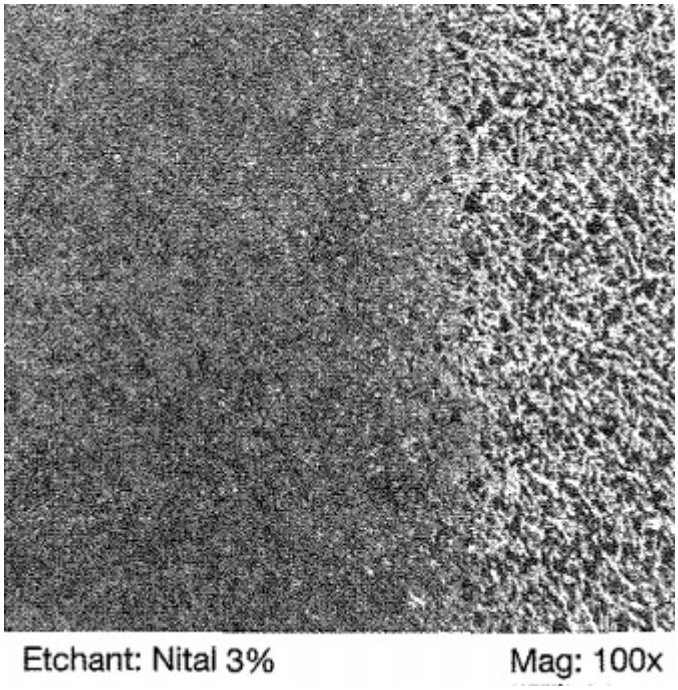


Figure 3.14. QTB rebar case and core.

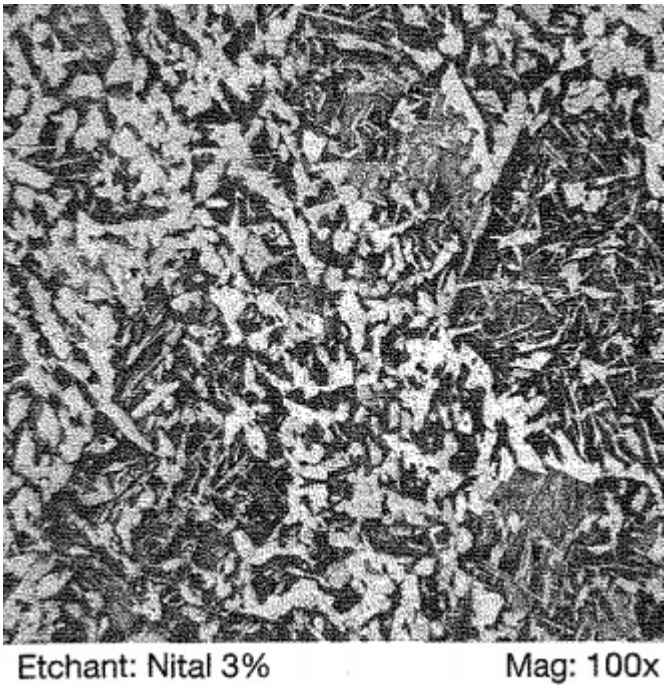


Figure 3.15. As-rolled rebar core.

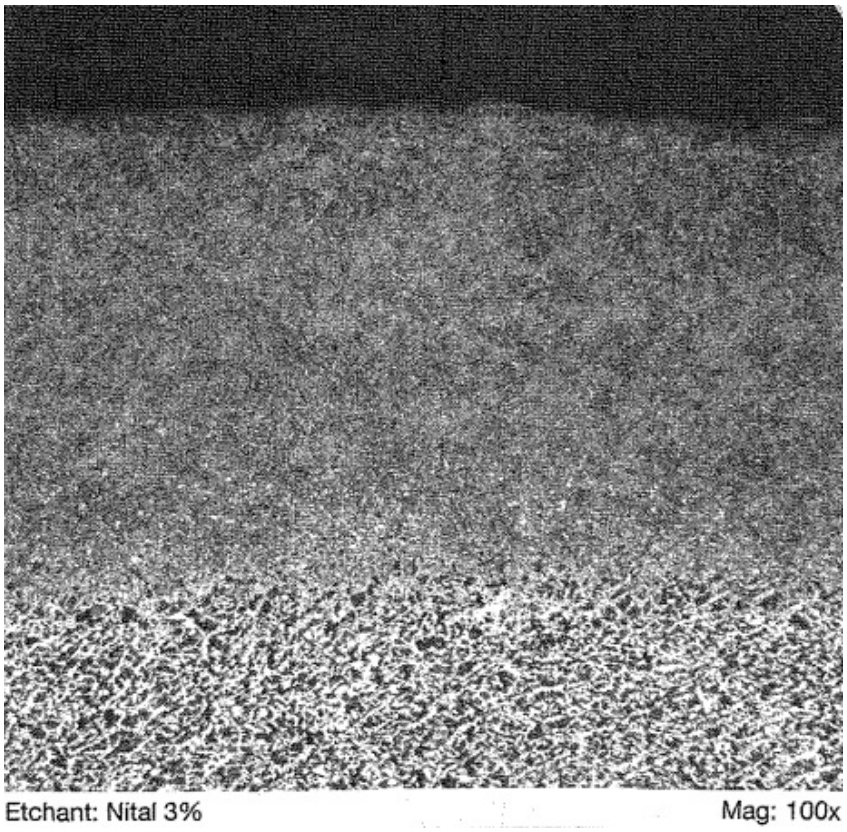


Figure 3.16. QTB surface, transition and core.

Implementation in production requires good water quality, a pumping system capable of handling the required volumes and pressures of water to achieve martensitic transformation, and a delivery system capable of evenly distributing water pressure and flow around the surface of the bar. Water must be delivered to the bar with enough pressure to prevent boiling of the water, generating steam at the bar surface. The part responsible for water delivery is commonly called a "cooler." Figure 3.17 is a schematic showing the water delivery to the bar for one cooler. The cooler shown in Figure 3.17 is supplied with highpressure water and is capable of sustaining high flowrates of water. In practice, multiple coolers are placed in series in order to obtain the desired quenching power of the system, as shown in Figure 3.18. Water must be supplied with sufficient pressure to avoid steam generation — commonly called a "steam barrier." Steam acts as a thermal insulator and reduces the rate at which heat is extracted from the bar, which can prevent formation of martensite. Several considerations are needed to maintain effective quenching. A pumping system must, be installed that can maintain the pressure and flowrates to create martensite on the surface of the bar. Second, the coolers must be sized appropriately for the bar being produced. In general, the closer the cooler inside diameter (ID) is to the size of the bar being quenched, the more powerful the quenching effect will be. When sizing the coolers, the engineer must also consider the challenges of threading the bar through the tubes. For example, a 2-inch ID cooler will be ineffective quenching a У 2-inch bar. A 7/8-inch ID cooler will be difficult to repeatedly thread a 3/4-inch bar through. The quenching process starts when the bar enters the first tube. The next critical event is to provide the system with a definite stopping point to the quenching process. To do this, a different tube, called a "stripper," is installed in the quench box. The stripper functions the same way as a cooler, but the water is applied against the direction of travel instead of with it. The stripper uses a high-pressure water spray and air to blast any residual water off the bar, so that when the bar leaves the stripper, it begins its tempering phase. Without the strippers, the quenching process is impossible to control. Figure 3.19 is an illustration of the workings of a stripper.

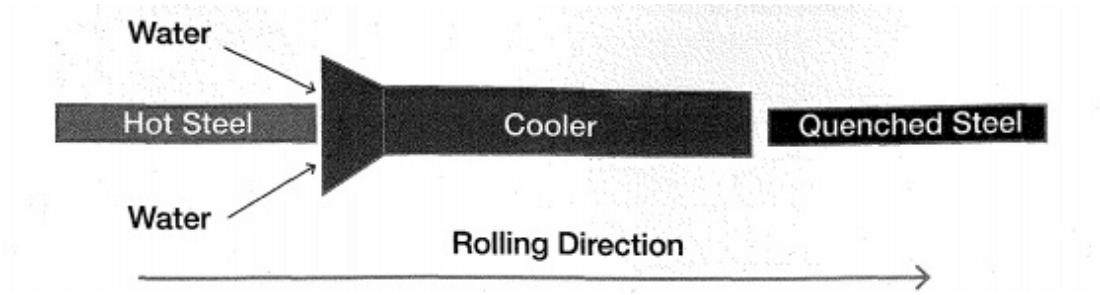


Figure 3.17. Representation of a functioning QTB cooler.

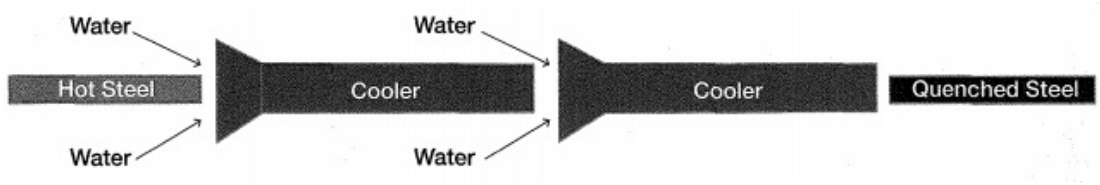
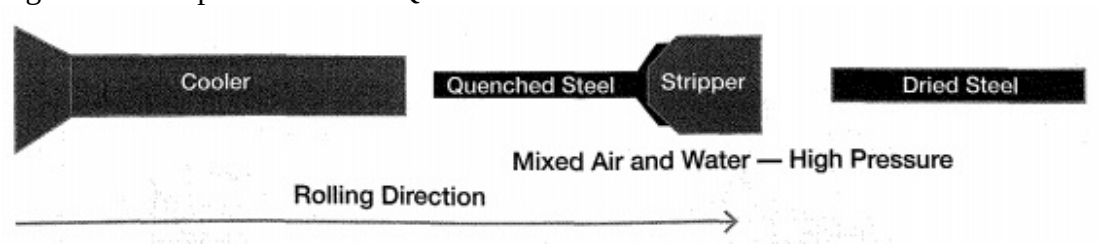


Figure 3.18. Representation of QTB coolers in series.



Fure 3.19. Representation of functioning QTB stripper.

The QTB process has many input variables that must be kept in control in order to deliver the desired results. Some of these input variables are: finishing temperature of the bar, number of coolers, number of strippers, water pressure, water flow, finishing speed and cooler size relative to bar size. However, the process has only one output variable — tensile properties. Assuming a steady chemistry, the primary determining factor of the strength of the bar is the depth of the quench. As such, measuring the tensile properties of the bar gives a very good indication of the quenching system's performance at any given moment. As is described later, tensile testing is a poor indicator of future performance unless all input variables are tightly controlled. The sum of all thermal inputs to the QTB process is the surface temperature of the bar as it leaves the quenching process. Anything that reduces quenching performance will result in an increase in surface temperature at the QTB exit. Anything that increases the quenching performance will result in a decrease in temperature at the QTB exit. Once the bar exits the quenching process, it reheats and

enters the tempering phase. During the tempering phase, the bar will reach a peak reheat temperature, commonly called the "tempering temperature," and will then naturally cool to ambient temperature. In addition to the exit temperature of the quenching process, the tempering temperature must also be monitored. Given a constant chemistry, quenching temperature and tempering temperature, the mechanical properties of the bar will be remarkably consistent. Any changes in temperature at any point in the process will appear as a change in bar strength. The control chart illustrates both the ability of the QTB process to deliver consistent bar strength over time and also how the strength of the bar can suddenly change with no indication from the control chart. Note that samples 1-16 stay within 2 ksi of 100 ksi, and sample 17 suddenly drops to 96 ksi. This indicates that something in the process shifted to a higher temperature, reducing the effectiveness of the quench. This also illustrates that simply measuring the tensile properties of the bar is not adequate to guarantee product quality or conformance to standards. When looking at longer-term data, the process is normal and relatively stable — even with some normal rolling process variation. A paradigm shift is required in the rolling operation. When running QTB, heats are not "made" or "missed" in the meltshop by the chemistry; they are "made" or "missed" in the heat treating, which is controlled by the rolling mill. As a result, process parameters that are normally not considered quality-related become quality parameters. For example, changes in finishing speed result in changes in tensile strength and yield strength. A paradigm shift is also required when setting internal grade specifications. QTB causes a higher increase in yield strength than tensile strength as it is applied. As a result, QTB causes a compression of the tensile-to-yield ratio when compared to a fully alloyed counterpart (Table 3.1). When setting process parameters, the grade requirements must be fully understood. In cases like A615 rebar, where only minimum yield strength is specified, the critical specification is the tensile strength. If the tensile strength is above minimum, the yield strength will be safely above minimum. Elongation is rarely a concern due to the grain refinement discussed above. In cases where there is a maximum yield strength specified, the process must be carefully designed and controlled to maintain

a consistent, on-target yield strength. When the tensile-to-yield ratio is specified, it becomes even more difficult to achieve the specification.

Table 3.1. Comporation of Typical Properties: QBT vs. Fully Alloyed A615, Grade 60 Rebar.

Process average sample	Carbon (no spec)	Manganese (no spec)	Tensile (min. 90 ksi)	Yield (min. 60 ksi)	Elongation (min. 9%)	T/Y ratio (no spec)
Fully alloyed	0.42%	1.00%	106 ksi	68 ksi	12%	1.56
QTB	0.26%	0.75%	103 ksi	86 ksi	15%	1.19

As mentioned above, the primary determining factor of the final properties of the bar is the quench depth.

The ideal quench depth for a good balance between strength and ductility is 0.035-0.050 inch tempered martensite case. In addition, care must be taken to maintain an even quench depth around the entire bar. The quench depth will generally not follow the surface deformation of the bar, but will find an average path through the bar and stay very consistent unless something happens to change the process. Figure 3.20 shows this for a 3/4-inch rebar. Note the increased thickness of the case at the longitudinal ribs and the very circular pattern of the transition line (circle added for emphasis) in the cross-section. Note also in the longitudinal section (Figure 3.21) that the quench depth does not follow the transverse ribs, but rather forms almost a straight line through the bar: When tensile testing, the bar will always break at its weakest point. There are fewer deformations where the mill markings are rolled into the rebar. When planning mechanical testing, samples must be chosen to put the mill markings between the grips so that the strength of the weakest part of the bar is measured. Finer pearlitic structure of the core of the bar compared to as-rolled, fully alloyed counterpart. Improved ductility at strength levels equal to or higher than the as-rolled counterpart. Absorb a wide range of residuals in the steel from variations in the scrap steel supply. Figure 3.20 Quench depth longitudinal section. There is typically a 2-3 ksi difference in strength between samples that are pulled to break within the mill markings and samples that are pulled to break outside the mill markings. Microhardness testing was performed on the crosssection of the bar to

determine the degree of hardening achieved by the QTB process. The testing found that the case is measurably harder than the core of the bar, but it is not hardened to the degree typically considered as true case hardening. The hardness of the core averaged 215 HK, or a Rockwell 92 HRB equivalent. The hardness of the case averaged 315 HK, or a Rockwell 30 HRC equivalent. The hardness of the case is limited by the carbon content of the steel and also the degree of self-tempering from the residual heat radiating out from the core of the bar.

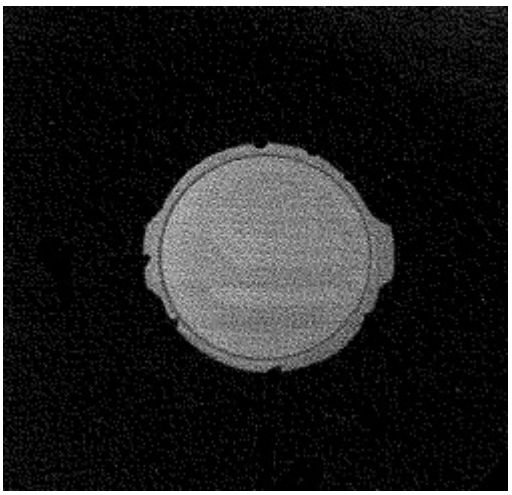


Figure 3.20. Quench depth cross-section.

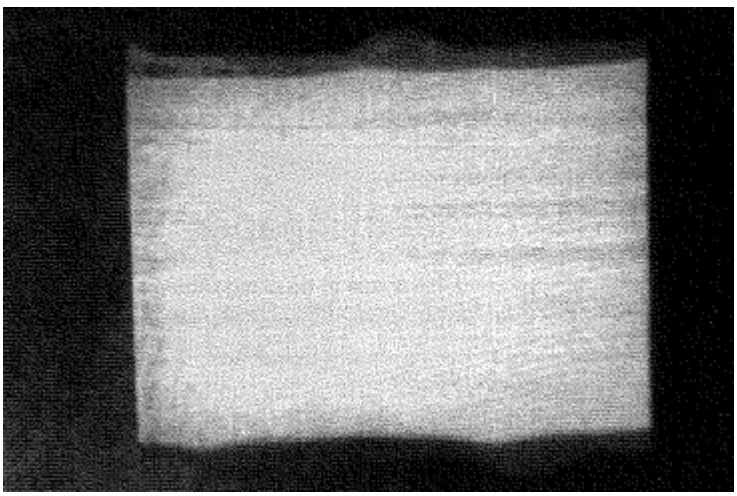


Figure 3.21. Quench depth longitudinal section.

QTB is an alternate means of strengthening long bars by quenching the bars with water and then allowing the bars to self-temper the hardened case. The process

is performed in-line with the rolling process, after the finishing stand. The process is stable and controllable.

3.1.2 Continuous Quenching Pipes

In this experiment 32 mm inner diameter and 4,9 meter length 4 thermex pipe was used. Total length of continuous quenching pipe is 19,6 meters. Figure 3.22 shows the schematic drawing of the pipe.

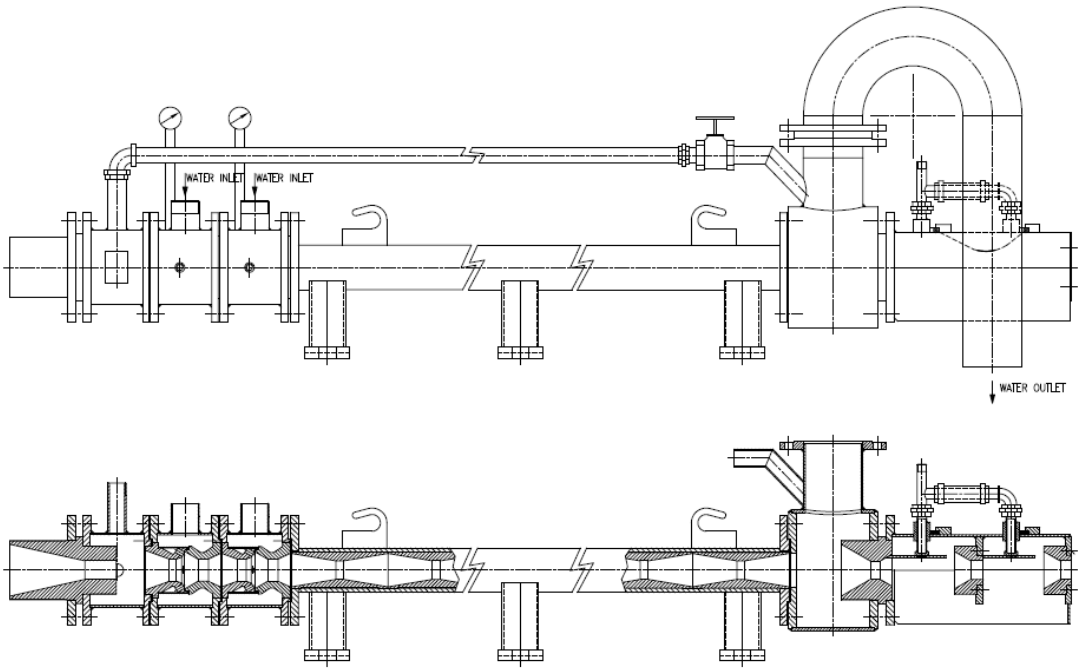


Figure 3.22. Schematic drawing of thermex pipe.

3.2. Hot Rolled Rebar and Standards

3.2.1 Overview of Rebar Standards

High-strength, low-alloy rebar is normally characterized by restricted carbon and carbon equivalent (CE) levels, greater ductility requirements, and controlled strength ranges. Many of the differences between rebar standards can be related to

the intended purpose and region that they were developed for, and relate mainly to the weldability and ductility properties of the steel.

Increasing the amount of carbon or other elements like manganese is a relatively cheap and easy way to increase the strength of steel. Unfortunately, it has a negative effect on ductility and weldability. Ductility is an important aspect in the design of earthquake resistant structures. Also important in seismic design is the ability to accurately predict how a structure will behave under real world conditions. This is motivation for having a tightly controlled strength range (as opposed to requiring only a minimum level). Weldability on the other hand, is a desirable characteristic in rebar that allows for efficient prefabrication of reinforcing structures in workshops and durability during transportation and handling to the construction site. However, carbon and other elements impair the ability to effectively weld steel. To ensure weldability, a low level of carbon (< 0.3%) and CE (a weighted average of a group of elements that have a similar effect as carbon: <0.55%) is required. A conflict between these requirements arises due to the fact that reducing the carbon and CE levels to achieve the desired weldability and ductility properties, also has the effect of reducing the strength of the rebar. In order to achieve all the necessary requirements, alternative production processes such as microalloying or QST must be used. Amount of alloy element and strengths for different standards is shown in Table 3.2.

Table 3.2 Chemical Requirements of World Rebar Standards

	C	Mn	P	S	Si	CE*	Tensile, min [MPa]	Yield, min [MPa]
US (A 706)	0,30	1,5	0,035	0,045	0,50	0,55	550	420
Canada	0,30	1,6	0,035	0,045	0,50	0,55	625	500
Australia/NZD	0,22	-	0,050	0,050	-	0,49	575	500
Japan	0,32	1,8	0,040	0,040	0,55	0,60	620	490
Germany	0,22	-	0,050	0,050	-	0,50	550	500

3.2.2 Used Rebar Standard

In the United States, the International Building Code (IBC) which is adapted and enacted by state governments, references American Concrete Institute's standard

ACI 318 for the construction of structural concrete. In turn, ACI 318 references ASTM standards for rebar.

There are two ASTM standards for plain carbon rebar, A 615 and A 706. Both of these standards include similar groups of requirements such as: dimensions, chemical composition, and mechanical properties. However, the main difference between the two is that A 706 has controlled tensile properties (meaning both minimum and maximum values are specified) and greater restrictions to alloy levels. The motivation behind the development of standard A 706, including mention of the various organizations involved, is provided in the report from ACI Committee 439. As previously mentioned the strain-hardening ratio of 1.25 required by A 706 presents a challenge in the use of the quench and tempering process.

In this work GR60 ASTM A 615 USA standard 12 mm diameter hot rolled notched rebar steel was used. TABLE 3.3 shows dimensions, mechanical and chemical properties of ASTM A 615 standard for USA standards rebar steel.

Table 3.3 ASTM A 615 USA rebar steel standards

ASTM A 615 / METRIC SYSTEM REBAR STEEL WITH NOCH STANDARD

RATED DIAMETER mm.	WEIGHT		TRANSVERSE NOCH				LENGTHWISE NOCH				PITCH (mm)		NOCH DEPTH	
	Kg/m	Tolerance %	HEIGHT (mm)		WITH (mm)		HEIGHT (mm)		WITH (mm)					
			min.	max.	min.	max.	min.	max.	min.	max.	min.	max.	min.	max.
8	0,395	± 6	0,32	0,64	0,64	0,96	0,40	1,12	0,64	1,60	4,00	5,60	2,01	3,14
10	0,618		0,40	0,80	0,80	1,20	0,50	1,40	0,80	2,00	5,00	7,00	2,51	3,92
12	0,888		0,54	1,08	0,96	1,44	0,60	1,68	0,96	2,40	6,00	8,40	3,01	4,71
14	1,208		0,63	1,26	1,12	1,68	0,70	1,96	1,12	2,80	7,00	9,80	3,51	5,49
16	1,578		0,72	1,44	1,28	1,92	0,80	2,24	1,28	3,20	8,00	11,20	4,02	6,28
18	2,000		0,81	1,62	1,44	2,16	0,90	2,52	1,44	3,60	9,00	12,60	4,52	7,06
20	2,466		1,00	2,00	1,60	2,40	1,00	2,80	1,60	4,00	10,00	14,00	5,02	7,85
22	2,984		1,10	2,20	1,76	2,64	1,10	3,08	1,76	4,40	11,00	15,40	5,52	8,63
25	3,853		1,25	2,50	2,00	3,00	1,25	3,50	2,00	5,00	12,50	17,50	6,28	9,81
28	4,834		1,40	2,80	2,24	3,36	1,40	3,92	2,24	5,60	14,00	19,60	7,03	10,99
32	6,313		1,60	3,20	2,56	3,84	1,60	4,48	2,56	6,40	16,00	22,40	8,04	12,56
36	7,990		1,80	3,60	2,88	4,32	1,80	5,04	2,88	7,20	18,00	25,20	9,04	14,13
40	9,865		2,00	4,00	3,20	4,80	2,00	5,60	3,20	8,00	20,00	28,00	10,05	15,70

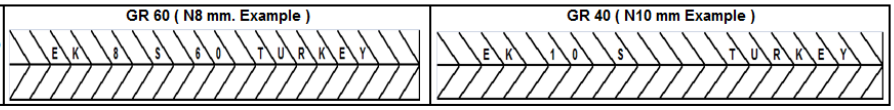
MECHANIC PROPERTIES

	GR 60	GR 40
YIELD STRENGTH (N/mm)	Min. 414	Min. 276
ULTIMATE STRENGTH (N/mm)	Min. 621	Min. 483
% ELONGATION Lo = 200 mm	8 ... 20 = Min 9	8 ... 10 = Min 11
	22 ... 25 = Min 8	12 ... 20 = Min 12
	28 ... 40 = Min 7	22 ... 40 = Min -

CHEMICAL COMPOSITION

ELEMENTS	GR 60	GR 40
% C	0,37 - 0,41	0,18 - 0,26
% Si	0,35 max.	0,25 max.
% S	0,060 max.	0,060 max.
% P	0,060 max.	0,060 max.
% Mn	0,95 - 1,20	0,60 - 0,95
% CE	-	-

NOCH GEOMETRY AND MARKING



PRODUCTION CHEMICAL ANALYSIS

QUALITY	C	Si	Mn	S	P	V	N	NOTE	QUALITY CODE
	0.	0.		0.0	0.0	0.0	max.		
GR 40	16-18	max. 20	0,55-0,60	45*	45*	-	0,015*	IKHH / 3/8"	EK 16/55
	20-22	max. 20	0,55-0,60	45*	45*	-	0,015*	OKHH / 4/8-5/8"-6/8"	EK 20/55
GR60	38-40	20-30	0,95-1,05	45*	45*	-	0,015*	N8-N10-3/8"	EK 38/95
	41-43	30-35	1,05-1,10	45*	45*	-	0,015*	N12-N20 / 4/8"-6/8"	EK 41/105
	41-43	30-35	1,00-1,10	45*	45*	07-09	0,015*	N22-N28 / 7/8"-9/8"	EK 41/100 + V
	41-43	30-35	1,00-1,10	45*	45*	09-11	0,015*	N32-N50 / 10/8"-18/8"	EK 41/100 + V
Thermex	20-22	max. 20	0,55-0,60	45*	45*	-	0,012*	N8 - N20	EK 20/55
Thermex	22-24	max. 20	0,55-0,60	45*	45*	-	0,012*	N12	EK 20/55
Thermex	20-22	max. 20	0,60-0,65	45*	45*	-	0,012*	N22 - N40	EK 20/60

As shown in table 3.3 minimum yield strength of rebar is 414 MPa and minimum ultimate tensile strength of rebar is 621 MPa. %0,20-0,22 carbon, %0,55-0,60 manganese and maximum %0,20 silicon must be used in this standard.

In this work %0,20 carbon, %0,58 manganese and %0,18 silicon was used as chemical alloy element. Result of yield strength of rebar was between 525 MPa to 599 MPa and ultimate tensile strength of rebar was between 624 MPa to 690 MPa.

3.3 Measuring Devices

3.3.1 Velocity Measurement of Liquid

Siemens SITRANS FM MAG 3100 electromagnetic flow meter was used to measure the liquid volume flow rate to calculate relative liquid velocity.

ITRANS F M MAG 3100 is an electromagnetic flow sensor with a large variety of liners, electrode material and with grounding electrodes as standard, all this ensures a perfect fit for almost every flow application. Also, measuring electrodes which are capable of withstanding the most extreme processes and various liners are available. The fully welded construction provides a ruggedness that fits almost every flow application.

Theory of operation;

The flow measuring principle is based on Faraday's law of electromagnetic induction.

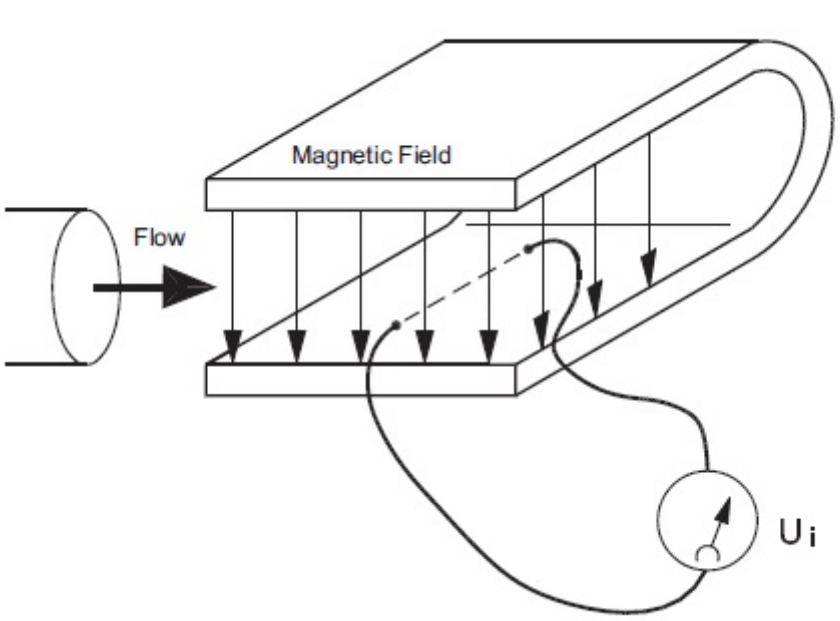


Figure 3.23 Magnetic field theories.

Ui = When an electrical conductor of length L is moved at velocity v, perpendicular to the lines of flux through a magnetic field of strength B, the voltage Ui is induced at the ends of the conductor

Ui = L x B x v

- Ui = Induced voltage
- L = Conductor length = Inner pipe diameter = k1
- B = Magnetic field strength = k2
- v = Velocity of conductor (media)
- k = k1 x k2

Ui = k x v, the electrode signal is directly proportional to the fluid velocity

Operating principle;

The coil current module generates a pulsating magnetizing current that drives the coils in the sensor. The current is permanently monitored and corrected. Errors or cable faults are registered by the self-monitoring circuit.

The input circuit amplifies the flow-proportional induced voltage signal from the electrodes.

The input impedance is extremely high: >1014 Ω which allows flow measurements on fluids with conductivities as low as 5 µS/cm. Measuring errors due to cable capacitance are eliminated due to active cable screening.

The digital signal processor converts the analog flow signal to a digital signal and suppresses electrode noise through a digital filter. Inaccuracies in the transmitter as a result of long-term drift and temperature drift are monitored and continuously compensated for via the self-monitoring circuit. The analog to digital conversion takes place in an ultra low noise ASIC with 23 bit signal resolution. This has eliminated the need for range switching. The dynamic range of the transmitter is therefore unsurpassed with a turn down ratio of minimum 3000:1.

3.3.2 Temperature Measurement of Steel Bar

LumaSense Technologies IMPAC IGA 5 Pyrometers was used to measure the temperature of steel bar.

IMPAC pyrometers are temperature measurement instruments that operate on the principle of infrared radiation, i.e. they detect infrared radiation of objects to determine the temperature.

In many industry sectors, the use of noncontact temperature measurement instruments is an important technology. For example, it is used for controlling complete factory processes or measuring even the smallest components to ensure a consistent quality level.



Figure 3.24. Picture of used pyrometer.

Table 3.4 Specification of the pyrometer

Instrument	IGA 5
Temperature ranges	250 - 3000°C
Spectral range	1.45 - 1.8 µm
Field of view (Minimum spot size Ø in mm)	optics F min 200 : 1 (min 1)
Exposure time (t90 1)	≤ 2 ms adjustable up to 10 s
Output	0/4 - 20 mA, RS232 or RS485, PIDcontroller (option)

Infrared Temperature Measurement;

The non-contact temperature measurement (pyrometry) is an optical measurement based on the property of all materials to send out electromagnetic radiation (infrared radiation). The infrared thermometer (pyrometer) uses this

radiation to determine the temperature. The pyrometer aims with the optics at a certain spot of the object and determines the temperature of this spot. Today typically spectral responses of pyrometers are in the near, middle and distant infrared.

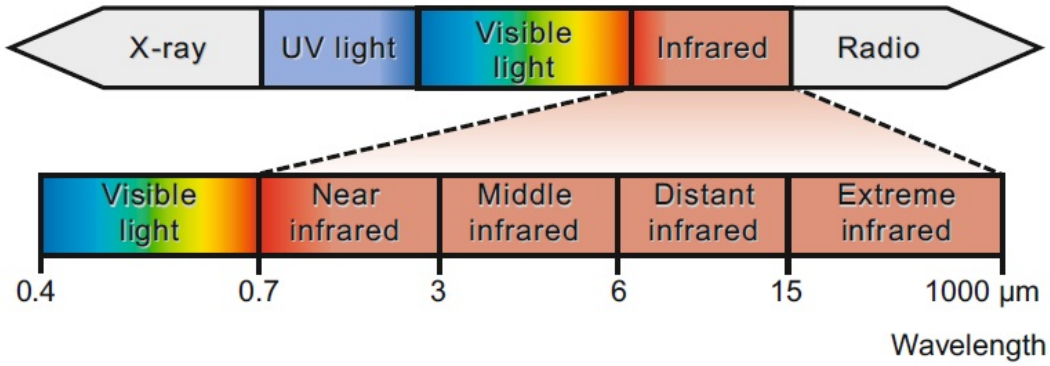


Figure 3.25 Electromagnetic spectrum

The material of the measured object demands the correct selection of the optimum spectral range of the pyrometer for a certain application. Therefore the correct spectral range is one of the most important features.

Typical spectral ranges are:

0.676 µm: Measurement of molten metals (min. 1100°C)

0.8 - 1.1 µm: Measurement of molten glass, metals, ceramics (min. 600°C)

1.45 - 1.8 µm: Measurement of metals, ceramics (min. 250°C)

2.0 - 2.8 µm: Measurement of metals (min. 50°C)

3 - 5 µm: Measurement of metals, ceramics (min. 5°C)

3.43 µm: Measurement of PE and PP foils (min. 50°C)

3.9 µm: Measurement in flame heated furnaces (min. 75°C)

5.14 µm: Measurement of glass surfaces (min. 100°C)

8 - 14 µm: Measurement of non-metal surfaces and coated metals (min. -40°C)

3.3.3 Temperature Measurement of Liquid

PT100 Thermo couple sensor was used to measure the liquid temperature. A thermocouple is a temperature-measuring device consisting of two dissimilar

conductors that contact each other at one or more spots, where a temperature differential is experienced by the different conductors (or semiconductors). It produces a voltage when the temperature of one of the spots differs from the reference temperature at other parts of the circuit. Thermocouples are a widely used type of temperature sensor for measurement and control, and can also convert a temperature gradient into electricity. Commercial thermocouples are inexpensive, interchangeable, are supplied with standard connectors, and can measure a wide range of temperatures. In contrast to most other methods of temperature measurement, thermocouples are self powered and require no external form of excitation. The main limitation with thermocouples is accuracy; system errors of less than one degree Celsius (°C) can be difficult to achieve.

Any junction of dissimilar metals will produce an electric potential related to temperature. Thermocouples for practical measurement of temperature are junctions of specific alloys which have a predictable and repeatable relationship between temperature and voltage. Different alloys are used for different temperature ranges. Properties such as resistance to corrosion may also be important when choosing a type of thermocouple. Where the measurement point is far from the measuring instrument, the intermediate connection can be made by extension wires which are less costly than the materials used to make the sensor. Thermocouples are usually standardized against a reference temperature of 0 degrees Celsius; practical instruments use electronic methods of cold-junction compensation to adjust for varying temperature at the instrument terminals. Electronic instruments can also compensate for the varying characteristics of the thermocouple, and so improve the precision and accuracy of measurements.

Specification; Probe 316 st/steel, 3 wire PFA lead, Class b element, -50 to + 250˚C, 1.5 m lead.

3.4 Mechanical Testing

Mechanical testing plays an important role in evaluating fundamental properties of engineering materials as well as in developing new materials and in controlling the quality of materials for use in design and construction.

Tensile testing, also known as tension testing, is a fundamental materials science test in which a sample is subjected to a controlled tension until failure. The results from the test are commonly used to select a material for an application, forquality control, and to predict how a material will react under other types of forces. Properties that are directly measured via a tensile test are ultimate tensile strength, maximum elongation and reduction in area. From these measurements the following properties can also be determined: Young's modulus, Poisson's ratio, yield strength, and strain-hardening characteristics. Uniaxial tensile testing is the most commonly used for obtaining the mechanical characteristics of isotropicmaterials. For anisotropic materials, such as composite materials and textiles, biaxial tensile testing is required.

A tensile specimen is a standardized sample cross-section. It has two shoulders and a gauge (section) in between. The shoulders are large so they can be readily gripped, whereas the gauge section has a smaller cross-section so that the deformation and failure can occur in this area.

The shoulders of the test specimen can be manufactured in various ways to mate to various grips in the testing machine (see the image below). Each system has advantages and disadvantages; for example, shoulders designed for serrated grips are easy and cheap to manufacture, but the alignment of the specimen is dependent on the skill of the technician. On the other hand, a pinned grip assures good alignment. Threaded shoulders and grips also assure good alignment, but the technician must know to thread each shoulder into the grip at least one diameter's length, otherwise the threads can strip before the specimen fractures.

In large castings and forgings it is common to add extra material, which is designed to be removed from the casting so that test specimens can be made from it. These specimens may not be exact representation of the whole workpiece because

the grain structure may be different throughout. In smaller workpieces or when critical parts of the casting must be tested, a workpiece may be sacrificed to make the test specimens. For workpieces that are machined from bar stock, the test specimen can be made from the same piece as the bar stock.

In this work ASTM A370 tension test standard was used and Dartec universal testing machine was used to obtain result of yield strength and ultimate tensile strength.

4. RESULT AND DISCUSSION

In this work GR60 USA quality standard 12 mm diameter notched hot rolled rebar steel was quenched different initial liquid temperature and different relative liquid velocity to see variation of material surface temperature, yield strength and ultimate tensile strength.

In first experiment, constant bar velocity, bar temperature, relative liquid velocity, liquid pressure and chemical composition was used to observe change of liquid temperature with bar surface temperature, yield and ultimate tensile strength.

In second experiment, constant bar velocity, bar temperature, initial liquid temperature, liquid pressure and chemical composition was used to observe change of relative liquid velocity with bar surface temperature, yield and ultimate tensile strength.

4.1. Experimental Result For Different Initial Liquid Temperature

In Figure 4.2, variation of initial liquid temperature with bar surface temperature are shown for the cooling of 12 mm diameter GR60 reinforcement steel bar with constant velocity, temperature, tube diameter and water velocity as shown in Table 4.1.

Table 4.1. Constant values for GR60 rebar steel.

Properties	**Value**
Bar diameter	N12
Quality Standard	GR60
Country Standard	USA (Metric)
Carbon %	0,20
Manganese %	0,56
Bar Velocity (m/s)	23,5
Bar surface temperature (^{o}C)	1090
Liquid pressure (Bar)	22
Liquid velocity (m/s)	42
Liquid volume flow rate (m^3/h)	90
Tube Diameter (mm)	30
Tube Length (m)	19,6

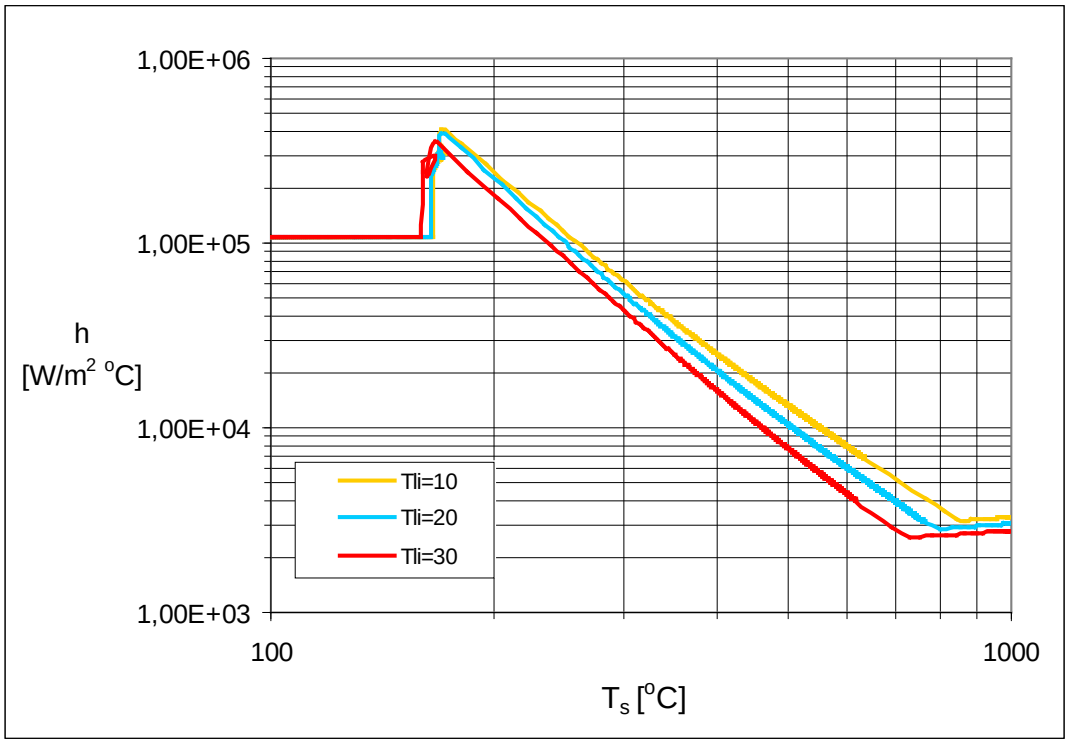


Figure 4.1. Variation of heat transfer coefficient with surface temperature for ANSI 1025 steel (u_l=35 m/s, u_b=5 m/s, d_b=18 mm, d_t=60 mm, $T_{s,initial}$=1000 ^oC)

Serin (2008) calculated variation of heat transfer coefficient with surface temperature for different initial liquid temperature for AISI 1025 steel bar. In Figure 4.1, variation of heat transfer coefficient with surface temperature and time respectively for different initial liquid temperatures are demonstrated for the cooling of 18 mm diameter cylindrical ANSI 1025 steel with the velocity of 5 m/s and 1000 ^oC initial temperature, 60 mm tube diameter and 35 m/s water velocity. Heat transfer coefficients at all boiling region, except forced convection and nucleate boiling regions, are dependent of initial liquid temperature, namely liquid subcooling and increase with the increase in liquid subcooling. Heat transfer coefficient and surface temperature of steel bar is affected by initial liquid temperature.

Serin (2008) also calculated variation of surface temperature with time for different initial liquid temperatures for the cooling of 18 mm diameter cylindrical ANSI 1025 steel with the velocity of 5 m/s and 1000 ^oC initial temperature, 60 mm tube diameter and 35 m/s water velocity. They took initial liquid temperatures as 10,

20 and 30 ^{o}C and time needed to cool the material from 1000 ^{o}C down to 200 ^{o}C varies from 3.3 seconds to 1.3 seconds for initial liquid temperatures 30 ^{o}C to 10 ^{o}C, respectively. As shown in Table 4.2, bar surface temperature measured in different liquid temperature from 21 ^{o}C to 28 ^{o}C and figure 4.1 shows the variation bar surface temperature with initial liquid temperature. As same as Serin (2008)'s works, bar surface temperature increase with increasing of initial liquid temperature respectively. Decreasing of initial liquid temperature from 28 ^{o}C to 21 ^{o}C effects on decreasing of surface temperature from 529 ^{o}C to 511 ^{o}C. This change also effect on increasing yield strength and ultimate tensile strength of steel bar.

Table 4.2 Experiment results for different initial liquid temperature.

Initial Liquid Temperature (^{o}C)	Bar Surface Temperature (^{o}C)	Yield Strength (MPa)	Tensile Strength (Mpa)
21	511	599	688
21	512	599	690
22	512	567	650
22	514	555	643
23	515	575	648
24	518	560	647
25	519	549	630
25	519	580	673
25	522	583	670
26	521	578	667
27	522	539	626
27	522	536	625
27	524	553	632
27	524	542	645
27	525	526	624
28	525	525	625
28	529	544	649

In Figure 4.2 increasing of surface temperature of steel bar depended of initial liquid temperature.

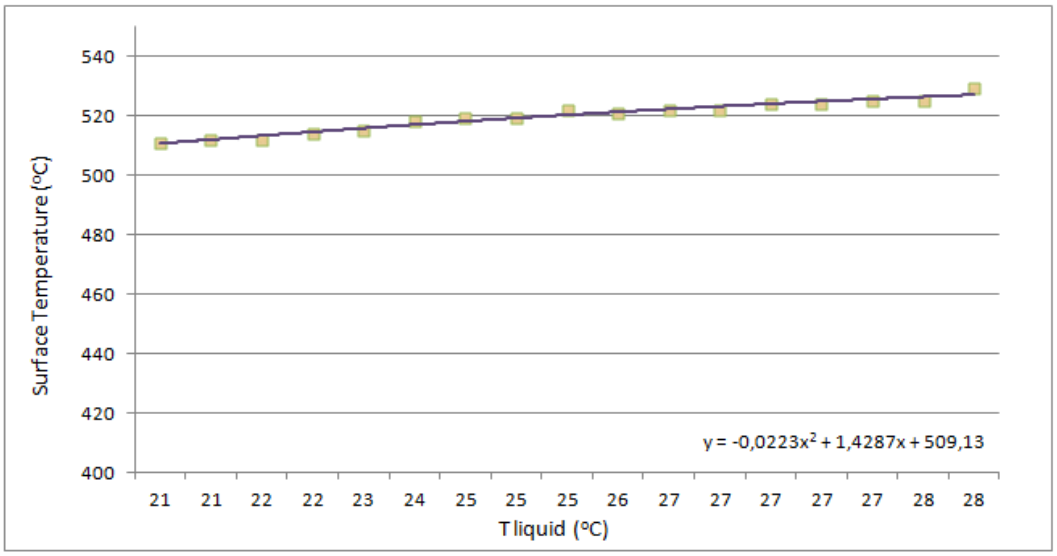


Figure 4.2. Variation of surface temperature with initial liquid temperature for GR60 steel bar.

In Figure 4.3, variation of yield strength and initial liquid temperature. Decreasing of initial liquid temperature effect on increasing of heat transfer coefficient and cooling rate result of increasing of yield strength. Decreasing of initial liquid temperature from 28 ^{o}C to 21 ^{o}C effects on increasing of yield strength from 525 ^{o}C to 599 ^{o}C. This change also effect on ultimate tensile strength of steel bar.

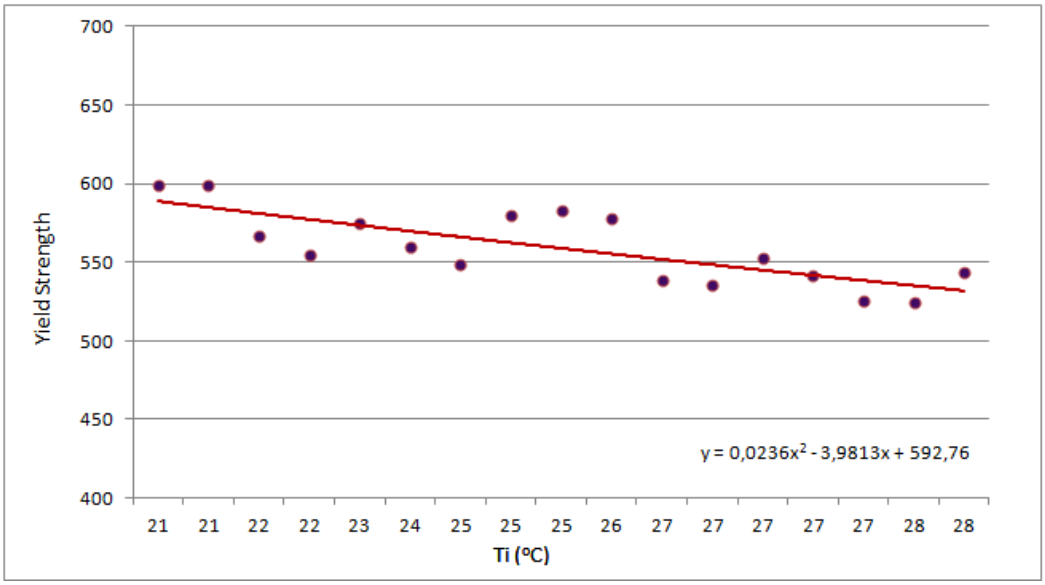


Figure 4.3. Variation of yield strength with initial liquid temperature for GR60 steel bar

In Figure 4.4, variation of tensile strength and initial liquid temperature. As same as Figure 4.3, Decreasing of initial liquid temperature effect on increasing of heat transfer coefficient and cooling rate result of increasing of tensile strength. Decreasing of initial liquid temperature from 28 ^{o}C to 21 ^{o}C effects on increasing of ultimate tensile strength from 525 MPa to 599 MPa.

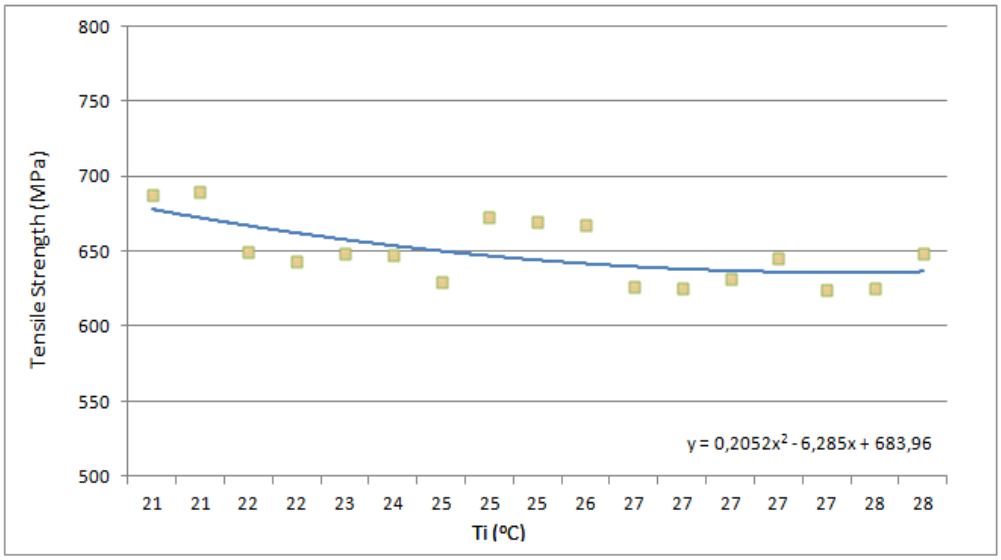


Figure 4.4. Variation of tensile strength with initial liquid temperature for GR60 steel bar.

4.2. Experimental Results For Different Relative Liquid Velocities

In this experiment relative velocity change from 15,5 to 21,5 to observe change of bar surface temperature, yield strength and ultimate tensile strength of GR60 steel bar. Constant values are shown in table 4.3.

Table 4.3. Constant values for GR60 rebar steel.

Properties	**Value**
Bar diameter	N12
Quality Standard	GR60
Country Standard	USA (Metric)
Carbon %	0,20
Manganese %	0,56
Bar Velocity (m/s)	23,5
Bar surface temperature (^{o}C)	1090
Liquid pressure (Bar)	22
Initial Liquid Temperature (^{o}C)	25
Tube Diameter (mm)	30
Tube Length (m)	19,6

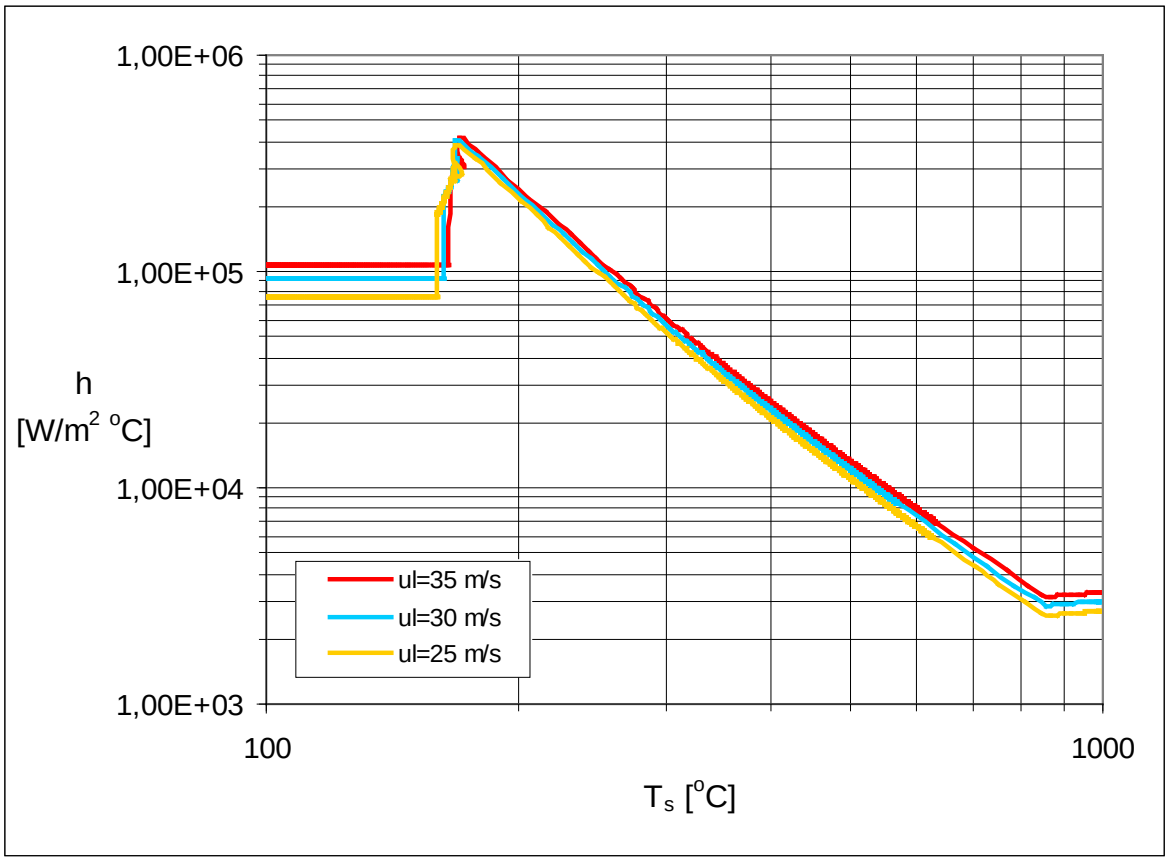


Figure 4.5. Variation of heat transfer coefficient with surface temperature for ANSI 1025 steel (u_b=5 m/s, d_b=0.018 m, d_t=0.060 m, $T_{l,initial}$=10 ^{o}C, $T_{s,initial}$=1000 ^{o}C)

Serin (2008) calculated variation of heat transfer coefficient with surface temperature for different relative liquid velocity for AISI 1025 steel bar. Figure 4.5 shows the effect of liquid velocity on heat transfer coefficient. Liquid velocities ranged from 25 to 35 m/s. In these figures, the velocity of cylindrical bar and the tube diameter are taken as 5 m/s and 60 mm, respectively. As shown in Figure 4.5, heat transfer coefficients at all boiling region are dependent of liquid velocity and increase with the increase in liquid velocity. The critical heat transfer coefficient and forced convection heat transfer coefficient are higher for higher liquid velocities and the intersection temperature between nucleate boiling and forced convection is obtained higher for higher liquid velocities as shown in Figure 4.5.

Serin (2008) also calculated the effect of liquid velocity on surface temperatures of cylindrical bar. Liquid velocities ranged from 25 to 35 m/s. Time needed to cool the material from 1000 ^{o}C down to 200 ^{o}C varies from 1.3 seconds to 1.8 seconds for liquid velocities 35 m/s to 25 m/s, respectively. As shown in Table 4.3, bar surface temperature measured in different relative liquid velocity from 15,5 m/s to 21,5 m/s and Figure 4.6 shows the variation of bar surface temperature with relative liquid velocity. As same as Serin (2008)'s works, bar surface temperature increase with increasing of initial liquid temperature respectively. Increasing of relative liquid velocity from 15,5 m/s to 21,5 m/s effects on decreasing of surface temperature from 525 ^{o}C to 510 ^{o}C. This change also effect on yield strength and ultimate tensile strength of steel bar.

Table 4.4. Experiment results for different relative liquid velocities.

Water Flow Rate (m^3/h)	Water Velocity (m/sn)	Relative Velocity (m/s)	Bar Surface Temperature (^oC)	Yield Strength (MPa)	Tensile Strength (MPa)
84	39	15,5	525	560	649
84	39	15,5	514	565	656
86	40	16,5	518	564	647
86	40	16,5	522	563	651
88	41	17,5	521	569	642
88	41	17,5	519	567	654
88	41	17,5	516	570	651
90	42	18,5	517	577	670
90	42	18,5	519	580	673
92	43	19,5	513	576	665
92	43	19,5	517	578	664
92	43	19,5	511	581	665
94	44	20,5	514	584	664
94	44	20,5	516	582	674
94	44	20,5	517	579	677
96	45	21,5	512	583	680
96	45	21,5	510	586	681
96	45	21,5	513	585	674

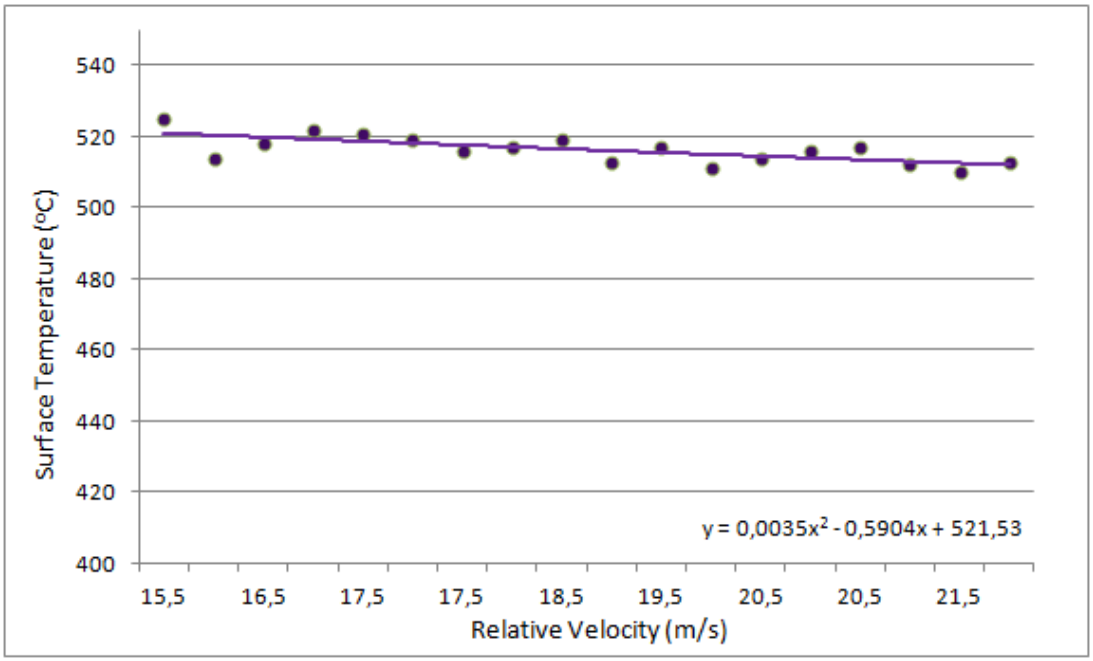


Figure 4.6. Variation of surface temperature with relative velocity for GR60 steel bar.

In Figure 4.7, variation of yield strength and liquid velocity. Decreasing of liquid velocity effects on increasing of heat transfer coefficient and cooling rate result of increasing of yield strength. Increasing of relative liquid velocity from 15,5 m/s to 21,5 m/s effects on increasing of yield strength from 560 MPa to 586 MPa. This change also effect on ultimate tensile strength of steel bar.

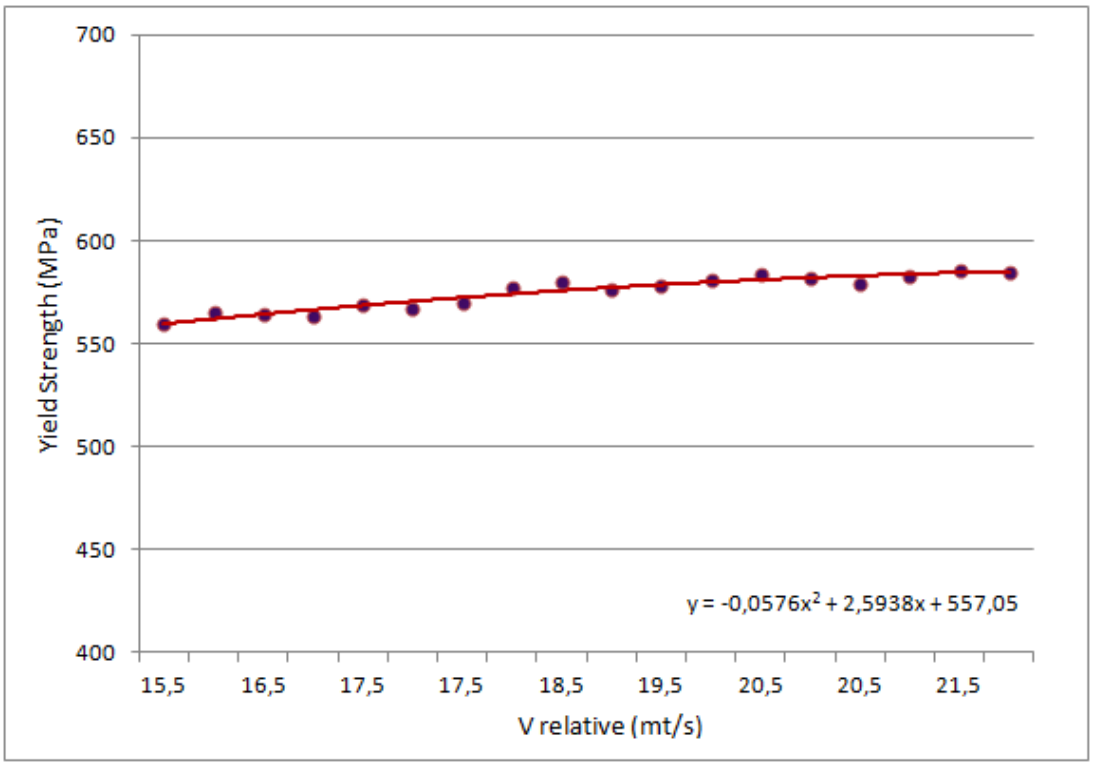


Figure 4.7. Variation of yield strength with relative velocity for GR60 steel bar

In Figure 4.8, variation of tensile strength and liquid velocity. As same as Figure 4.9, increasing of liquid velocity effects on increasing of heat transfer coefficient and cooling rate result of increasing of tensile strength. Increasing of relative liquid velocity from 15,5 m/s to 21,5 m/s effects on increasing of ultimate tensile strength from 642 MPa to 681 MPa.

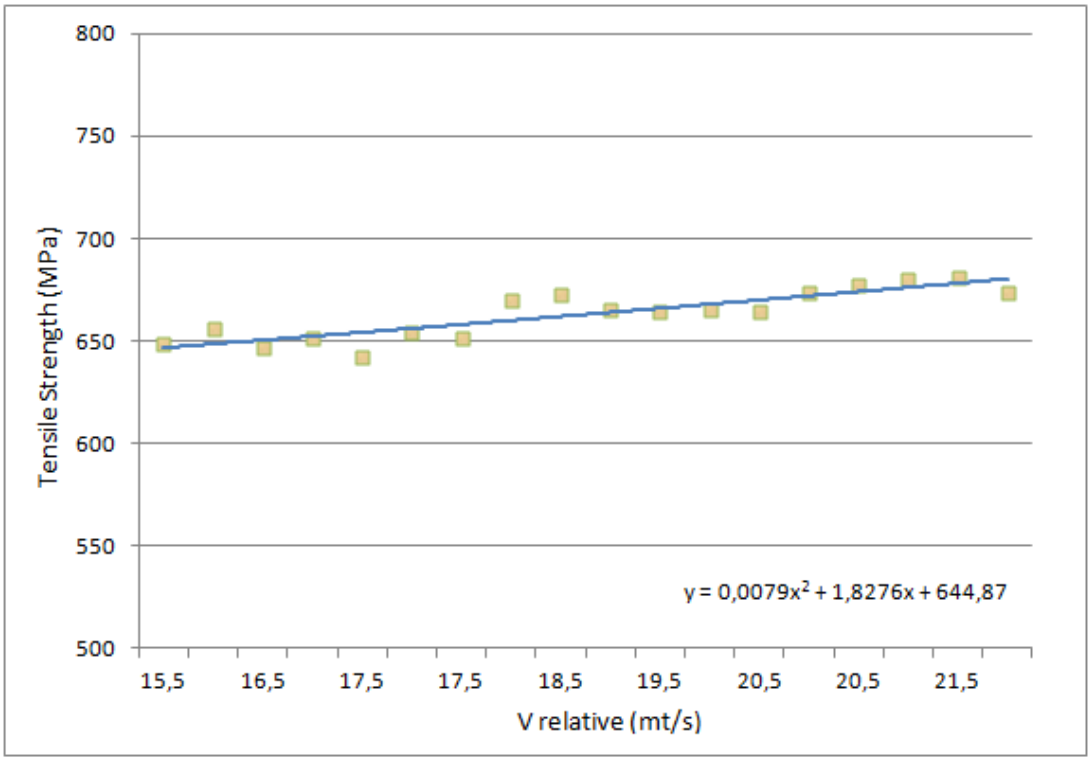


Figure 4.8. Variation of tensile strength with relative velocity for GR60 steel bar

5. CONCLUSIONS AND RECOMMENDATIONS

5.1. Conclusions

In this work, 12 mm diameter ASTM A 615/GR60 reinforcing steel was quenched under different initial liquid temperatures and different relative velocities conditions to see variation of material surface temperature, yield strength and ultimate tensile strength. Quenching of steel is important in iron and steel industry. Better control of quenching means is better quality of steel and less power requirement on quenching process.

The effect of initial liquid temperature on quenching process, yield strength and ultimate tensile strength are investigated. Weather temperature depends on cooling performance of liquid. Experiments were performed different season to provide of temperature difference.

It is seen that decreasing of initial liquid temperature from 28 oC to 21 oC directly effect on increasing yield strength from 525 MPa to 599 MPa and ultimate tensile strength from 624 MPa to 690 MPa. Each 1 ^{o}C decreasing in temperature cause to 9,4 MPa increase of yield strength and as same as 10,5 MPa ultimate tensile strength respectively. This result shows that decreasing of liquid temperature result of increasing heat transfer, cooling rate and increasing amount of martensitc structure.

The effect of initial liquid velocity on quenching process, yield strength and ultimate tensile strength are investigated. Water velocity depends on volume flow rate of water. More pump power is had to use to increase volume flow rate. Experiments were performed different liquid volume flow rate to provide of relative liquid velocity difference.

Increasing relative liquid velocity from 15,5 m/s to 21,5 m/s directly effect on increasing in yield strength from 560 MPa to 586 MPa and ultimate tensile strength from 642 MPa to 681 MPa. Each 1 m/s increasing in relative velocity cause to 4,3 MPa increase of yield strength and as same as 6,5 MPa ultimate tensile strength

respectively. This result shows that increasing of relative liquid velocity result of increasing heat transfer, cooling rate and increasing amount of martensitc structure.

5.2. Recommendations for future works

This work shows that quenching is one of the important processes of heat treatment to improve the performance of steel in iron and steel industry. The investigation of quenching of steel with water, the effects of velocity and subcooling during cooling of steel, the different heat transfer coefficients for boiling regions, surface temperature of steel and water temperature is of great interest.

In this thesis, the temperature profiles in rebar steel under quenching boundary conditions are investigated. All future work involving thermal process of iron and steels need this knowledge to be used in analyses and calculations.

In future wok, it is recommended that the effect of initial liquid temperature and liquid velocity on micro structure of rebar steel.

REFERENCES

H. CETINEL, ET AL., 2000. A Finite Element Based Prediction Of The Microstructural Evolution Of Steel Subjected To The Tempcore Process, Mechanics Of Materials 32, Pp. 339-347.

J. NIKOLAOU, ET AL., 2004. Microstructures And Mechanical Properties After Heating Of Reinforcing 500 Mpa Class Weldable Steels Produced By Various Processes (Tempcore, Microalloyed With Vanadium And Work – Hardened), Construction And Building Materials 18, Pp. 243-254.

L. J. MALVAR, 1998. Review Of Static And Dynamic Properties Of Steel Reinforcing Bars Aci. Mater J; 609-616, September-October.

H. ZHENG, A. A. ABEL, 1998. Stress Concentration And Fatigue Of Profiled Reinforcing Steels. Int J Fatigue 20(10), Pp. 767-773.

T. HELGASON, J. M. HANSON N. F. SOMES, W. GENE COORLEY AND E. HOGNESTAD, 1976. Fatigue Strength Of High-Yield Reinforcing Bars. National Cooperative Highway Research Program, Report 164, Transportation Research Board, National Research Council, Washington DC.

H. ZHENG, A. A. ABEL, 1999. Fatigue Properties Of Reinforcing Steel Produced By Tempcore Process. J Mater Civil Eng 11(2), Pp. 158-165.

P. BALA, J. PACYNA, J. KRAWCZYK, 2007. The Influence Of The Kinetics Of Phase Transformations During Tempering On The Structure Development In A High Carbon Steel. Archives Of Metallurgy And Materials. I, Pp. 113-120.

P. BALA AND J. PACYNA, 2008. The Influence Of Pre – Tempering On The Mechanical Properties Of Hs6-5-2 High Speed Steel, Archives Of Metallurgy And Materials 53, 3, Pp. 795-802.

P. BALA, 2009. The Kinetics Of Phase Transformations During Tempering Of Tool Steels With Different Carbon Content, Archives Of Metallurgy And Materials 54, 2, Pp. 491- 498.

SAGE AM., 1976. Effect Of Vanadium, Nitrogen, And Aluminium On The Mechanical Properties Of Reinforcing Bar Steels. In: Winterton House High Street, Editor. Vanitec, Metals Technology. Kent: Westerham, Pp. 65–70.

GLODOWSKI RJ., 2000. Effect Of V And N On Processing And Properties Of Hsla Strip Steels Produced By Thin Slab Casting. In: Iron And Steel Society, Editor. Proceedings Of 42nd Mechanical Working And Steel Processing Conference, 38. Canada: Toronto, Pp. 1–10.

BAKKALOGLU A., 2002. Effect Of Processing Parameters On The Microstructure And Properties Of An Nb Microalloyed Steel. Mater Lett;56(3):200, Pp. 1–9.

REHM G., RUSSWURM D., 1977. Assessment Of Concrete Reinforcing Bars Made By The Tempcore Process. Metall Rep C.R.M. No. 51, Pp. 3–16.

SIMON P, ECONOMOPOULOS M AND NILLES P. 1984. Tempcore: A New Process For The Production Of High Quality Reinforcing Bars. Iron Steel Eng;61(3):53–7.

ECONOMOPOULOS M, RESPEN Y, LESSEL G AND STEFFES G., 1975. Application Of The Tempcore Process To The Fabrication Of High Yield Strength Concrete–Reinforcing Bars. Metall Rep C.R.M. No. 45, Pp. 1–17.

CSA STANDARD CAN/CSA-G30.18-M92, “Billet-Steel Bars For Concrete Reinforcement,” Standards Council Of Canada, Ottawa, On, 1992.

JAPANESE INDUSTRIAL STANDARD JIS G 3112:2004, “Steel Bars For Concrete Reinforcement,” Japanese Standards Association, Tokyo, 2005.

AUSTRALIAN/NEW ZEALAND STANDARD AS/NZS 4671:2001, “Steel Reinforcing Materials,” Standards Australia, Sydney, Australia, And Standards New Zealand, Wellington, New Zealand, 2001.

ASTM STANDARD A 615/A 615M-09, “Standard Specification For Deformed And Plain Billet-Steel Bars For Concrete Reinforcement,” Astm International, West Conshohocken, Pa, 2009, Doi: 10.1520/A0615_A0615m-09b, Www.Astm.Org.

MATTHEW ALLEN, 2011. An Investigation Of The Suitability Of Using Aisi 1117 Carbon Steel In A Quench And Self-Tempering Process To Satisfy Astm A

706 Standard Of Rebar. Master Of Applied Science, Graduate Department Of Materials Science And Engineering University Of Toronto.

A. MUKHOPADHYAY, L.M. GALASSON, M. ENA AND GBUZZI, 2010. An Investigation Of The Suitability Of Using Aisi 1117 Carbon Steel In A Quench And Self-Tempering Process To Satisfy Astm A 706 Standard Of Rebar. Danielli Automation.

MAGALLON D., HUHTINIEMI I. 2001. CORIUM MELT QUENCHING TESTS AT LOW RESSURE AND SUBCOOLED WATER IN FARO. Nuclear Engineering And Design 204, Pp. 369–376.

UTTARA PRASAD, QIANG XU, MAHESH C. CHATURVEDI, 2002. Effect Of Cooling Rate And Manganese Concentration On Phase Transformation In Ti–45 At.% Al Based Alloys. Materials Science And Engineering A329–331,

D.V. EDMONDSA, K. HE, F.C. RIZZO, B.C. DE COOMAN, D.K. MATLOCK, J.G. SPEER, 2006. Quenching And Partitioning Martensite—A Novel Steel Heat Treatment. Materials Science And Engineering A 438–440, Pp. 25–34.

AHMED ISMAIL ZAKY FARAHAT, S.A. EL-BADRY, 2009. Effect Of High Temperature Deformation And Different Cooling Rates On Microstructure And Mechanical Properties Of Fe–Al Alloys. Materials Science And Engineering A 525, Pp. 48–54.

A.I. ZAKY, A. EL-MORSY, T. EL-BITAR, 2009. Effect Of Different Cooling Rates On Thermomechanically Processed High-Strength Rebar Steel. Journal Of Materials Processing Technology 2 0 9, Pp. 1565–1569.

B.K. PANIGRAHI, S. SRIKANTH, AND G. SAHOO, 2009. Effect Of Alloying Elements On Tensile Properties, Microstructure, And Corrosion Resistance Of Reinforcing Bar Steel. Journal Of Materials Engineering And Performance, Volume 18(8) November 2009, Pp. 1102-1108.

JACOB SELZER, 2012. Quenched And Tempered Bar. The Iron & Steel Technology Conference And Exposition, Atlanta, Ga., And Published In The Conference Proceedings.

ÖZGEÇMİŞ

He was born on 08/12/1981 in Mersin. He studied primary and high school in Mersin. He started Çukurova University Engineering Faculty Mechanical Engineering Departmen in 2000 and graduated in 2006. In same year, he started Master of Science at Mechanical Engineering Automotive Department. He started to work private sector in 2007 and he obligated to interrupt Master of Science. He continued Master of Science in 2012 and graduated in 2015. He is still working at a special firm in iron and steel sector.